In presenting this dissertation as a partial fulfillment of the requirements for an advanced degree from the Georgia Institute of Technology, I agree that the Library of the Institution shall make it available for inspection and circulation in accordance with its regulations governing materials of this type. I agree that permission to copy from, or to publish from, this dissertation may be granted by the professor under whose direction it was written, or, in his absence, by the Dean of the Graduate Division when such copying or publication is solely for scholarly purposes and does not involve potential financial gain. It is understood that any copying from, or publication of, this dissertation which involves potential financial gain will not be allowed without written permission.

Benjamin L. Kittle

ABRUPT ENLARGEMENTS IN CIRCULAR PIPES

A THESIS

Presented to the

Faculty of the Graduate Division

By

Benjamin L. Kittle

In Partial Fulfillment

of the Requirements for the Degree

Master of Science in Civil Engineering

Georgia Institute of Technology

August 1956

6 s
12 R

ABRUPT ENLARGEMENTS IN CIRCULAR PIPES

Approved:

____

____

____

Date Approved by Chairman: November 30, 1957

ACKNOWLEDGMENTS

The writer is grateful to Professor C. E. Kindsvater for his guidance and assistance as thesis director; to Professors M. R. Carstens and W. R. Metcalfe for their service as members of the reading committee; to Mr. Homer J. Bates, laboratory technician; to Mr. Jack Davidian for his assistance in the laboratory; and to the U. S. Geological Survey for material assistance in making this work possible.

TABLE OF CONTENTS

LIST OF TABLES

LIST OF FIGURES

SUMMARY

Fluid flow from a smaller into a larger pipe through an abrupt area enlargement is accompanied by separation, high shear stresses between the expanding stream and the surrounding fluid, extreme velocity gradients, and exceptional turbulence downstream from the enlargement. The abnormal flow persists over a considerable length of the larger pipe before the normal uniform flow pattern is restored. The total energy loss in the section of pipe containing the enlargement and the disturbed flow is assumed to consist of two parts: that due to the resistance of the boundary walls and that due to separation and the formation of a turbulent wake in the expansion reach downstream from the enlargement. The magnitude of the total energy loss as well as the relative size of its two components depends on the relative size of the enlargement, the shape and relative roughness of the pipe, the Reynolds number of the flow, and the turbulence characteristics and velocity distribution of the entering stream.

The purpose of this study was to determine the energy loss that occurs at abrupt enlargements in smooth pipes and to separate the total loss into its two components. Six enlargement ratios were used in the experiments. A range of Reynolds numbers from 1×10^4 to 1×10^6 was investigated. A special series of tests involved the use of an expanded-metal sleeve, six inches long and equal in outside diameter to the inside diameter of the pipe. This sleeve was placed immediately downstream from

the enlargement to determine the effect of roughness on the two components of the total energy loss.

The larger of the two energy losses in the region of flow establishment downstream from an abrupt enlargement is (H_B), which is that part due to turbulence in the wake. This loss is primarily dependent on boundary geometry, which is expressed in terms of the area-enlargement ratio, A_2/A_1. This loss can be determined by application of the Borda-Carnot equation. The remainder of the total energy loss (H_f') is attributed to boundary resistance. Its magnitude depends on the enlargement ratio, the Reynolds number of the flow, the relative roughness of the pipe, flow conditions at the entrance, and the distance over which the total loss is measured.

The conclusions drawn from the experimental data were based on an evaluation of the total energy loss (H_L) and the apparent boundary resistance loss (H_f') in the first 25 diameters of the pipe downstream from the enlargement. This length is believed to be sufficient to contain the major part of the non-uniform flow.

The customary procedure for computing the total energy loss in a pipe line containing an abrupt enlargement is to add the loss computed from the Borda equation to the boundary-resistance loss. From the results of the experiments it was concluded that the customary procedure will give results which are as accurate as is justified by the measurements on which the computations are based. For values of the enlargement ratio greater than 2.32 the loss computed by the Borda equation was only 2 to 3 percent larger than the difference between the measured total loss and the computed boundary-resistance loss.

In general, the experimental results confirm the hypothesis that the total energy loss is reduced by boundary roughness in the region immediately downstream from the enlargement.

CHAPTER I

INTRODUCTION

Description of the Problem.--The flow of a fluid from a smaller into a larger pipe through an abrupt enlargement is characterized by separation, high shear stresses between the expanding stream and the surrounding fluid, extreme velocity gradients, and exceptional turbulence downstream from the enlargement. The abnormal flow persists over a considerable length of the larger pipe before the normal uniform flow pattern is restored. A large portion of the total energy possessed by the fluid entering the expansion is converted into heat by the viscous shear stresses occurring at the interface between the jet and the surrounding fluid. A smaller amount is converted into energy of turbulence, which is eventually dissipated as heat during the decay of the excess turbulence. The remainder of the energy of the entering stream accrues to the total energy of the uniform flow downstream from the enlargement.

The total energy loss that occurs at an abrupt enlargement has been assumed to consist of two parts: that due to the resistance of the boundary walls and that due to separation and the formation of a turbulent wake in the expansion reach downstream from the enlargement. The magnitude of the total energy loss as well as the relative size of its two components depends on the relative size of the enlargement, the shape and relative roughness of the pipe, the Reynolds number of the flow, and the turbulence characteristics and velocity distribution of the entering stream.

Purpose and Scope of the Study.--The purpose of the experimental phase of this investigation was to determine the energy loss that occurs at abrupt enlargements in smooth, circular pipes. Major objectives of the analysis were to separate the total energy loss into its two components and to determine the effect of an obstruction in the eddy zone surrounding the entering stream.

Enlargements used in the experiments were abrupt and symmetrical. The downstream pipe used was three inches in diameter. Six degrees of enlargement were used for the tests on the smooth pipe. For a special series of tests, an expanded-metal sleeve, six inches long and equal in outside diameter to the inside diameter of the pipe, was placed immediately downstream from the enlargement. Non-uniform velocity distribution and turbulence in the entering stream were largely eliminated by the use of short, smooth nozzles instead of a smaller pipe upstream from the enlargement. All enlargement tests were made for high Reynolds numbers, corresponding to flow in the turbulent range. The boundary-resistance characteristics for uniform flow in the test pipe were determined for a full range of Reynolds numbers. Laboratory measurements included the rate of flow and complete piezometric traverses for each test.

Review of Previous Research on Abrupt Enlargements.--The traditional method of computing the energy loss occurring at an abrupt enlargement in a pipe involves the application of the Borda (or Borda-Carnot) equation,

$$H_B = \frac{(V_1 - V_2)^2}{2g} = (\frac{A_2}{A_1} - 1)^2 \frac{V_2^2}{2g} , \qquad (1)$$

in which H_B is the energy loss due to the enlargement, V_1 and V_2 are the average velocities, and A_1 and A_2 are the areas of the small pipe and the large pipe, respectively. The Borda equation is derived by the simultaneous solution of the one-dimensional energy and momentum equations applied to a length of pipe extending from the enlargement to a section of uniform flow. The effect of boundary resistance is neglected in the derivation of the Borda equation. In practice, the total energy loss in a pipe containing an abrupt enlargement is usually computed as the sum of the enlargement loss and the normal boundary resistance loss in the pipe sections adjacent to the enlargement.

Many investigators have attempted to verify the Borda equation experimentally. Notable among these were A. H. Gibson (1)(2) and W. H. Archer (3). Neither of these investigators took into account the influence of upstream flow conditions, the Reynolds number of the flow, or the relative roughness of the boundaries.

Gibson's tests covered area ratios (A_2/A_1 = ratio of downstream pipe area to upstream pipe area) from 2.25 to 10.96. Gibson reported that a coefficient should be applied to the Borda equation to make it agree with his experiments. For a value of $A_2/A_1 = 10.96$ he recommended a coefficient of 1.04. For decreasing values of the area ratio he recommended decreasing values of the coefficient. Thus, for $A_2/A_1 = 2.25$ the coefficient derived from Gibson's tests was 0.95.

Archer's tests covered values of A_2/A_1 from 1.45 to 9.32. Based on his experiments, he also recommended the use of coefficients with the Borda equation. Archer furnished a table of coefficients which involved a considerable extrapolation of his test results. For A_2/A_1 = infinity, the coefficient recommended by Archer was 0.75. For $A_2/A_1 = 1.25$, he recommended 1.22. Thus, Archer contradicted Gibson by indicating that the coefficient for the Borda equation increases with the enlargement ratio.

A more recent study, concerned primarily with the mechanism of energy transformation at an abrupt enlargement, was that performed by A. A. Kalinske (4). Kalinske's tests, which covered only two rates of flow and one enlargement ratio, give much information on the relationship of the mean velocity distribution, energy dissipation, and the growth and decay of the turbulent wake. From his tests, Kalinske concluded that the principal energy loss occurs at the interface between the entering jet and the eddying fluid in the separation zone. This loss was attributed to the extreme shear stresses at the interface. The turbulence energy produced in the wake was shown to be a small part of the total energy transformation. The maximum ratio of turbulence energy to mean kinetic energy was 0.50. Kalinske also demonstrated that velocity distribution upstream from the enlargement has considerable influence on the energy loss in the enlargement.

Another recent study was reported by Schütt (5). Schütt's experiments involved the use of polished nozzles to give four enlargement ratios. His experimental data consisted mainly of piezometric profiles. Schütt concluded from his tests that the normal flow pattern is virtually restored at a distance of eight pipe diameters downstream from the enlargement. His results indicated that the Borda equation, without any experimental adjustment, can be used to compute the energy loss at an abrupt enlargement.

This conclusion was based on the observation that measured values of head loss for all test conditions differed by less than one percent from values computed by the Borda equation.

~~A noteworthy part of Schütt's investigation consisted of tests made with the corner eddy zone downstream from the enlargement completely filled with a solid material to produce a gradual enlargement. When he compared the results of these tests with the tests on abrupt enlargements he was unable to establish a relationship between the eddy zone and the total energy loss. However, he did find that the diffusion process was completed in a shorter length of pipe when the gradual enlargement was used.~~ From the results of his piezometric measurements in the vicinity of abrupt enlargements Schütt was also able to verify the assumption, basic to the derivation of the Borda equation, that the pressure on the annular area at the face of the enlargement is equal to the pressure in the smaller pipe.

The writer's investigation is the second on this topic to be conducted at the Georgia Institute of Technology. The first was a thesis investigation by Fleetwood (6) in 1955. Fleetwood's experiments covered two degrees of pipe roughness, four area-enlargement ratios, and a maximum Reynolds number range of from 1.5×10^4 to 4.0×10^5. He used smooth, lucite nozzles to produce the smaller stream at the enlargement. Two pipes were used. Both pipes were constructed of polished, transparent lucite, and both were 6 inches in diameter by 15 feet in length. His smooth pipe was made up of flange connected, three-foot lengths. Irregularities in the walls and mis-matching at the joints actually prevented this pipe from being hydraulically smooth. Fleetwood'd rough pipe was made by gluing gravel to the wall of the lucite pipe.

The average enlargement ratios (A_2/A_1) tested by Fleetwood were 1.8, 3.4, 6.9, and 17.5. The Reynolds number range covered by tests on the different pipes and nozzles was limited by the head and discharge available. Piezometric profiles were recorded for all tests. A limited number of velocity traverses were made in the nozzles as well as the pipes.

The procedure used by Fleetwood to separate the total energy loss into two components consisted of subtracting the computed enlargement loss (Borda equation) from the total loss in the first 25 diameters of pipe downstream from the enlargement. The principal conclusions drawn from his experiments were:

a. The boundary resistance loss depends on the enlargement ratio, the Reynolds number, the relative roughness of the pipe, flow conditions at the entrance, and the length of the nominal flow-expansion reach over which the total head loss is measured.

b. The boundary resistance loss is influenced only slightly by the Reynolds number, but very much by the enlargement ratio and relative roughness.

c. The influence of the enlargement ratio is greater for smooth pipe than for rough pipe.

d. For both smooth and rough pipe, and for enlargement ratios less than four the boundary friction loss in the expansion reach is slightly smaller than the corresponding uniform-flow resistance loss in the same reach. For larger values of the enlargement ratio, the boundary resistance loss becomes larger than that for uniform flow.

e. In comparison with the total energy loss downstream from an abrupt enlargement, the difference between the actual boundary resistance loss and that computed for uniform flow is insignificant.

It was concluded from Fleetwood's tests that the boundary resistance loss increases with the enlargement ratio and, for enlargement ratios greater than three, that the loss is greater for smooth pipes than for rough pipes. At an enlargement ratio of seventeen, for example, the boundary resistance loss for the smooth pipe was twelve times larger than that for the rough pipe. It should be emphasized, of course, that all of the conclusions above are based on an arbitrary definition of the boundary loss as the residual obtained by subtracting the computed expansion loss from the measured total loss in the first 25 pipe diameters downstream from the enlargement.

CHAPTER II

THEORETICAL CONSIDERATIONS

The Borda Equation.--One of the classic equations of fluid mechanics is the Borda-Carnot equation for the energy loss caused by an abrupt enlargement in a pipe. The Borda equation, as it is usually called, is derived from the one-dimensional energy and momentum equations. It is derived without regard for the boundary shear stresses. Therefore, it does not recognize the possible influence of boundary resistance. Furthermore, it does not account for the influence of transverse velocity distribution in the adjacent pipe sections. When it is applied to the problem of determining the total head loss in a pipe system, it is assumed to represent a loss of energy which is in addition to the normal boundary resistance loss.

Figure 1* is a definitive sketch for the flow of a fluid through an abrupt enlargement. Section 1 is immediately downstream from the enlargement. Section 2 is in a uniform-flow region of the downstream pipe. In the traditional derivation of the Borda equation, the following assumptions are made:

a. The flow in section 2 and in the jet at section 1 is steady and uniform. This means that velocity vectors are parallel and that the piezometric head is constant in both cross-sections.

---

*Figures and tables are contained in the Appendix.

b. The piezometric head in the separation zone surrounding the jet at section 1 is the same as the piezometric head in the jet. It is assumed that the live stream issuing from the small pipe persists without change in velocity, energy, or momentum into the region immediately downstream from the expansion.

c. The tangential force due to boundary resistance between sections 1 and 2 is negligible.

As applied to the fluid freebody between sections 1 and 2, the momentum principle of fluid mechanics requires that the summation of the external forces acting on the freebody in the direction of motion be equal to the change in the momentum flux of the fluid within the limits of the freebody. Thus,

$$\Sigma F_s = Q \rho (V_2 - V_1), \tag{2}$$

in which ΣF_s is the summation of all external forces acting in the direction of motion, Q is the total discharge, V is average velocity, and ρ is the mass density.

As indicated in Figure 1, the external forces acting are the forces due to pressure (F_1 and F_2) and the s-component of force due to fluid weight (F_g). From the figure

$$F_1 = p_1 A_2 = p_1 \frac{\pi D_2^2}{4},$$

and

$$F_2 = p_2 A_2 = p_2 \frac{\pi D_2^2}{4},$$

in which p_1 and p_2 are the average pressures at sections 1 and 2, respectively, A_2 is the area and D_2 is the diameter of the larger pipe, assumed to be circular. The force due to fluid weight (F_g) is

$$F_g = W \sin \theta = \gamma L_2 A_2 \frac{(z_1 - z_2)}{L_2} ,$$

$$= \gamma (z_1 - z_2) \frac{\pi D_2^2}{4} ,$$

in which $(z_1 - z_2)$ is the difference in elevation in the length L_2 along the axis of the pipes, and γ is the specific weight of the fluid. Substituting in equation 2, the summation of external forces is

$$\Sigma F_s = F_1 - F_2 + F_g = p_1 \frac{\pi D_2^2}{4} - p_2 \frac{\pi D_2^2}{4} + \gamma (z_1 - z_2) \frac{\pi D_2^2}{4}$$

or

$$\Sigma F_s = \left[(p_1 - p_2) + \gamma (z_1 - z_2) \right] \frac{\pi D_2^2}{4} .$$

The change in momentum flux is

$$Q \rho (V_2 - V_1) = A_2 V_2 \rho (V_2 - V_1) = \rho V_2 (V_2 - V_1) \frac{\pi D_2^2}{4} .$$

Substituting the last two equations in equation 2, dividing by γ, and simplifying,

$$\left(\frac{p_1}{\gamma} + z_1\right) - \left(\frac{p_2}{\gamma} + z_2\right) = \frac{V_2}{g} (V_2 - V_1),$$

in which the left side of the equation is the difference in piezometric head. Substituting the symbol h for the piezometric head ($p/\gamma + z$), the momentum equation has the form

$$h_1 - h_2 = \frac{V_2}{g}(V_2 - V_1). \tag{3}$$

The one-dimensional energy equation written to describe the flow between sections 1 and 2 is

$$\left(\frac{V_1^2}{2g} + h_1\right) - H_B = \left(\frac{V_2^2}{2g} + h_2\right), \tag{4}$$

from which the difference in total energy between sections 1 and 2 is equal to the loss in energy due to the enlargement (H_B). Solving equations 3 and 4 simultaneously,

$$H_B = \frac{(V_1 - V_2)^2}{2g}, \tag{1}$$

which is the Borda equation.

Modification of the Borda Equation.--By including the boundary resistance force in the summation of forces acting in the direction of motion, Fleetwood (6) derived the equation,

$$\left(\frac{V_1^2}{2g} + h_1\right) - \left(\frac{V_2^2}{2g} + h_2\right) = \frac{(V_1 - V_2)^2}{2g} + f'\,\frac{L_2}{D_2}\,\frac{V_2^2}{2g}, \tag{5}$$

in which the left side is the difference in total energy, H_L, the first term on the right is equivalent to the Borda equation, and the second term is a quantity which can be defined as the head loss due to boundary resistance, $H_f{}'$. If the Borda equation is assumed to represent the energy loss caused by the enlargement, then

$$H_f{}' = H_L - H_B = f' \frac{L_2}{D_2} \frac{V_2^2}{2g} . \tag{6}$$

Thus, the loss attributed to the effect of boundary resistance in the reach downstream from an abrupt enlargement is represented by an equation which is similar to the Darcy equation for uniform flow in circular pipes,

$$H_f = f \frac{L}{D} \frac{V_2^2}{2g} . \tag{7}$$

In equation 6 and 7, f' and f are functions of pipe roughness and the pipe Reynolds number. However, f' is also a function of L_2, because the flow in the reach between sections 1 and 2 is non-uniform. In the analysis of his tests, Fleetwood computed H_L, $H_f{}'$, and f' on the basis of a constant value of $L_2/D_2 = 25$. This length was believed to be sufficient to contain the non-uniform flow downstream from the enlargement.

CHAPTER III

LABORATORY SETUP

General.--The laboratory tests for this investigation were made in the Hydraulics Laboratory, School of Civil Engineering, Georgia Institute of Technology. The arrangement of laboratory equipment is shown in Figures 2 and 3.

The piping was arranged so that the constant-head recirculating system could be used for tests involving the smaller discharges. For larger rates of flow the constant-head system was by-passed with a pipe line connected directly to a pump. The maximum rate of flow used in the tests was 1.33 cubic feet per second.

The approach portion of the test section consisted of a short length of twelve-inch diameter pipe equipped with straightening vanes and baffles at the upstream end to reduce velocity non-uniformities and angularity. The rate of flow was controlled by a gate valve located in the 3-inch pipe downstream from the test section. This arrangement ensured full flow in the test pipe for all discharges.

Test Pipe.--The pipe used for the experiments consisted of a twenty-foot length of 3-inch diameter extruded aluminum pipe. It is shown in Figure 3. The inside of the test pipe had been ground with a cylinder hone to obtain a smooth surface and to make the pipe as nearly circular and cylindrical as possible. The diameter of the pipe was measured with a cylinder gage, accurate to one thousandth of an inch. The diameter was measured on two axes (90° apart) and at 60 sections over the length of the pipe. The average of these measurements was used as the inside diameter of the pipe for all computations.

Entrance Section for Boundary Resistance Tests.--A smooth, rounded entrance was placed at the upstream end of the test pipe for the boundary resistance tests. This entrance was used to prevent flow separation and turbulence at the transition from the 12-inch approach pipe to the 3-inch test pipe. The entrance piece was fabricated from wood, sanded smooth, and painted. The circular portion of the entrance piece was carefully matched to the test pipe to prevent disturbances resulting from mismatching. Figure 4 shows details of the rounded entrance.

Nozzles.--Nonuniformities in the velocity of the stream entering the test pipe were reduced by using short, smooth nozzles instead of smaller pipes. Six nozzles were used for a full range of enlargement ratios. The largest nozzle was approximately four inches long. The smaller nozzles were shorter, but the cylindrical portion on all nozzles was at least one inch long. Figure 5 shows the nozzles used in the tests. Details and dimensions of the nozzles are given in Figure 6. Figures 7 and 8 show a typical nozzle installed in the entrance section.

Great care was taken in the construction of the nozzles, particularly to insure that the downstream portions were perfect cylinders. The nozzles were made from solid aluminum stock. They were polished smooth. Each nozzle was equipped with four piezometers. The inside diameter of the cylindrical part of the nozzles was determined as the average of several measurements with an inside micrometer.

Rough Sleeve.--For a special series of tests, a sleeve, six inches in length, was inserted in the upstream end of the test pipe, adjacent to the nozzles. The location of the sleeve is shown in Figure 7. Details of the sleeve are shown in Figure 9.

The sleeve was made from a single piece of 1/4-inch by 18-gauge unflattened expanded metal. Portions of the metal fabric were cut and bent inward approximately one fourth of an inch as shown in Figure 9. The sleeve was held in place with a short bolt placed in a hole drilled through one side of the test pipe.

Instrumentation.--Piezometers were installed in quadruplicate in the nozzles and at 14 sections along the length of the test pipe. The piezometer holes were one-sixteenth of an inch in diameter, drilled perpendicular to the pipe wall and honed to prevent burrs at the inside surface. Figure 7 shows the location of piezometers in the nozzles, and Table 1 shows the location of piezometer sections in the test pipe. The average pressure at each section was obtained by manifolding the four piezometers to a single manometer connection.

Piezometric heads were measured with precision manometers. Due to the wide range of pressures involved in the tests it was necessary to use three different manometers. For low pressures, an air-water differential manometer reading to one thousandth of a foot was used. For intermediate pressures, a water-mercury differential manometer reading to one thousandth of an inch was used. Because a few pressures at the highest discharges were beyond the range of these two manometers, it was necessary to use another water-mercury manometer having a maximum differential of five feet. This manometer could be read to one hundredth of a foot, with thousandths estimated. For large deflections the relative accuracy of the larger manometer was comparable to that obtained with the smaller manometers.

Discharge Measurements.--Weighing-tank equipment was used to measure the volume-rate of flow for all tests. Measurements included weight, time, and water temperature. Weights were measured with a platform-beam scale to the nearest pound. Time intervals were measured to the nearest one hundredth of a second with an electric stop clock. The laboratory weighing equipment is fully automatic, eliminating the possibility of human errors in measuring weights and time intervals.

CHAPTER IV

EXPERIMENTAL PROCEDURE

Boundary Resistance Tests.--The uniform-flow resistance characteristics of the test pipe were determined as a basis for comparison with the abrupt-enlargement tests. Sixteen tests were made. The results are shown in Figure 10.

The arrangement of equipment for the boundary resistance tests was described in Chapter III. The tests involved measurements of the discharge and piezometric profiles for a range of values of the Reynolds number as limited by the water supply. Values of the hydraulic gradient used to compute the resistance coefficient (f) in the Darcy equation (equation 7) were determined as the slopes of lines fitted to the downstream, straight portions of the piezometric profiles. The test pipe was 80 diameters long. The entrance to the test section from the 12-inch approach pipe was rounded. Results of tests by Shapiro and Smith (14) indicate that normal values of the resistance coefficient were attained in the downstream portion of the pipe. It is assumed, therefore, that the values of f shown in Figure 10 correspond to the condition of uniform flow.

Abrupt Enlargement Tests.--A total of 74 tests were made with abrupt enlargements at the entrance to the test pipe. This number included tests on six enlargement ratios (A_2/A_1), from 1.49 to 16.53. The lowest value of the Reynolds number for any test was 1×10^4, and the maximum value was 1×10^6. Eighteen of the total number of tests, involving three different enlargement ratios, were made with the sleeve (Figure 9) located at the entrance to the test section.

The test procedure consisted of measuring the discharge and determining the piezometric-head profile for each setup. Data for the piezometric-head profiles were obtained from measurements of the difference between the piezometric head (h) at each of the piezometer sections in the pipe and the piezometric head (h_1) at the piezometer section in the nozzle. From these data a dimensionless ratio consisting of ($h-h_1$) divided by the approximate mean velocity head in the pipe ($V_2^2/2g$) was computed. The piezometric head ratio was then plotted on a large sheet of cross-section paper as a function of the distance of the measurement section from the enlargement section (L/D_2 in dimensionless form), and a smooth profile was drawn through the plotted points. Figure 11 shows a typical profile.

Table 2 shows values of the ratio $\Delta h/(V_2^2/2g)$ which were read from the piezometric profiles. Here $\Delta h = (h_2-h_1)$ is the difference in piezometric head between the beginning of the enlargement and a section which is 25 pipe diameters downstream. From this ratio values of Δh were computed for use in determining the loss of total energy in the nominal expansion reach.

The 25-diameter distance used for evaluating the total energy loss was selected for several reasons. This was the distance used by Fleetwood in the analysis of his tests, primarily because his test pipes were only slightly more than 25 diameters in length. It was demonstrated in his tests that a value of $L/D_2 = 25$ was sufficient to contain most of the non-uniform flow resulting from the enlargement. Thus, the velocity distribution was compared with that from the Kármán-Prandtl equations, and the hydraulic gradient at the end of the 25-diameter reach was compared with the corresponding hydraulic gradient for uniform flow. The results confirmed the conclusions drawn by Kalinske (4), who demonstrated that the excess turbulence due to the enlargement is virtually dissipated in the first 17 diameters of the pipe.

CHAPTER V

SUMMARY AND ANALYSIS OF TEST RESULTS

Summary of Boundary-Resistance Tests.--The results of the boundary resistance tests are shown in Figure 10. Also plotted on this diagram are the results of tests made by Schnabel (7) and others on the same pipe. The dashed curve drawn through the experimentally determined values was used for computations requiring the normal value of the Darcy resistance coefficient (f, equation 7) for the test pipe. The figure shows a comparison of this curve with the Kármán-Prandtl curve for smooth boundaries and a typical Colebrook-White curve for pipes with non-uniform roughness. The curve used for the writer's investigation gives values of f which are 3 to 4 percent higher than the values given by the Kármán-Prandtl equation for hydraulically smooth pipes.

Summary of Abrupt-Enlargement Tests.--The principal results of the tests on abrupt enlargements are shown in Table 2 and Figures 12 to 17, inclusive. Table 2 is a summary of measured and computed data. The column headings and some of the equations involved in the computation of quantities listed in Table 2 are explained in notes appended to the table. Figures 12 to 17, inclusive, are plots of the total-energy loss coefficient (C_L) as a function of the Reynolds number ($\underline{R}_2$) of the flow in the pipe. Here C_L is defined as $H_L/(V_2^2/2g)$, in which H_L is the measured loss of total energy in the 25-diameter reach downstream from the enlargement. Each of the different figures represents a different value of the enlargement ratio (A_2/A_1). Figures 12, 14, and 16 show the results of tests with the smooth pipe only. Figures 13, 15, and 17 include the results of special tests with a sleeve (Figure 9) immediately downstream from the enlargement.

To indicate the relative portion of the total-energy loss which might be attributed to boundary friction, a horizontal line is shown in Figures 12 to 17, inclusive. The value of the coefficient (C_B) which defines this line is computed from the Borda equation. Thus, from equation 1,

$$H_B = \frac{(V_1 - V_2)^2}{2g} = \left[\frac{A_2}{A_1} - 1\right]^2 \frac{V_2^2}{2g} = C_B \frac{V_2^2}{2g} ,$$

or,

$$C_B = \left[\frac{A_2}{A_1} - 1\right]^2 , \qquad (8)$$

from which C_B is a function of the enlargement ratio alone. The difference between the measured total loss and the loss computed from the Borda equation can be attributed to boundary resistance. Thus, H_f' is defined as the residual loss charged to boundary resistance,

$$H_f' = H_L - H_B ,$$

or,

$$C_f' = \frac{H_f'}{V_2^2/2g} = C_L - C_B . \qquad (9)$$

Values of C_f' are given in Table 2. They are also represented by the vertical distance between the curves of C_L and C_B in Figures 12 to 17, inclusive.

The negative slope which is characteristic of all the experimentally derived curves of C_L indicates that the total-loss coefficient decreases with increasing values of the Reynolds number. Because the enlargement-loss coefficient (C_B) is constant for any one value of the enlargement ratio, it follows that the boundary-resistance coefficient (C_f') also decreases with increasing values of the Reynolds number. This is not unexpected, because the magnitude of the Darcy coefficient (f) for smooth pipes in the same range of Reynolds numbers is known to vary inversely with the magnitude of $\underline{R}_2$, and (f) can be related to a coefficient (C_f) which is directly comparable with (C_f'). Thus, from the Darcy equation for uniform flow (equation 7),

$$H_f = f \frac{L}{D} \frac{V_2^2}{2g} = C_f \frac{V_2^2}{2g} ,$$

or,

$$C_f = f \frac{L}{D} . \tag{10}$$

Values of C_f, computed from equation 10, with f from Figure 10 and L/D_2 = 25, are shown in Table 2. A graph of C_f as a function of $\underline{R}_2$ is shown in Figure 12. It cannot be shown in the other figures in this group because of the limits of the vertical scales in Figures 13 to 17, inclusive.

An alternate method of summarizing the results of the abrupt-enlargement tests consists of subtracting the normal boundary resistance loss from the total loss to obtain a residual loss which might be attributed to the enlargement. Thus, if H_x is this residual loss,

$$H_x = H_L - H_f ,$$

or

$$C_x = \frac{H_x}{V_2^2/2g} = C_L - C_f , \tag{11}$$

in which C_x is an alternate enlargement-loss coefficient. Values of C_x are shown in Table 2. They are used in some of the subsequent analyses.

Analysis of the Test Results.--The results of the tests shown in Figures 12 to 17, inclusive, indicate certain trends which were unexpected and some which contradict the results obtained by Fleetwood. Figure 12, for an enlargement ratio of 1.49, shows total-loss coefficients which are somewhat larger than C_B for all values of $\underset{\sim}{R}_2$. At the other extreme, Figure 17, for an enlargement ratio of 16.53, shows a total loss coefficient which is considerably smaller than C_B. The trend indicated by these extremes is substantiated, in general, by Figures 13, 14, 15, and 16, although comparisons should take into account the difference in the vertical scales used on the several figures. Fleetwood, on the other hand, found that the total loss was always larger than that computed from the Borda equation.

The purpose of the special tests made with an expanded-metal sleeve in the pipe at the entrance to the test section was to determine the relative effect of retarding the eddy which forms in the corner zone adjacent to the enlargement. It had been suggested that these experiments might explain some of the questionable results attributed to the influence of pipe roughness in Fleetwood's investigation. Figure 13 shows that the total-loss coefficient is larger with the sleeve in place. However, Figures 15 and 17 show that the sleeve causes C_L to be smaller in comparison with the completely smooth pipe. Nevertheless the results of this investigation are not completely contradictory. It should be noted that Figure 13 shows the results for tests on a comparatively small enlargement ratio. The energy of the corner eddy is small in this instance, and the metal projections on the inside of the sleeve may have actually retarded the live stream entering the pipe. Thus, the effect of the sleeve could have been to increase the loss of energy at the enlargement.

On the other hand, Figures 15 and 17 show the results of tests with enlargement ratios of 6.48 and 16.53, respectively. For these tests, the kinetic energy of the eddy in the corner zone might have been an appreciable part of the total energy, and the effect of the sleeve could have been to retard the eddy, thus reducing the amount of flow energy required to sustain the eddy action. This suggests a possible verification of the hypothesis concerning the influence of pipe roughness at the entrance to the enlargement. In the preceding section (equation 9) C_f' was defined as an alternate coefficient of boundary resistance loss obtained by subtracting the enlargement-loss coefficient (C_B) from the total-loss coefficient (C_L). Also in this section (equation 10) C_f was defined as the boundary-resistance coefficient for uniform flow in the test pipe. The ratio C_f'/C_f is shown in Figure 18 as a function of $\underline{R}_2$ for all of the tests. The curves shown on Figure 18 provide a measure of the agreement between the alternate definitions for the loss of energy due to boundary resistance. It is apparent that the greatest disagreement between the two definitions occurs for the tests involving the largest enlargement ratio. It should be observed, however, that this is the condition for which the boundary resistance loss is the smallest in comparison with the total loss in the test reach. Therefore, it is also the condition for which C_f', being equal to the small difference between two large numbers, is subject to the greatest error.

The coefficient C_x was defined (equation 11) as the difference between C_L and C_f. Thus, C_x can be described as an alternate enlargement-loss coefficient for comparison with C_B from the Borda equation. The ratio C_x/C_B is shown for all of the tests on Figure 19. It is to be expected that, as shown on this figure, the greatest disagreement between C_x and C_B would occur for the smallest enlargement ratios, for which both H_x and H_B are least in comparison with H_L. Thus, the greatest disagreement between the alternate definitions occurs when the enlargement-loss, by either definition, is the least in comparison with the total loss. In other words, the comparisons shown in Figures 18 and 19 are somewhat misleading because they do not associate the difference between alternative definitions of the component losses with the magnitude of the total loss.

Figure 20 shows the relative magnitude of C_B or C_f as a function of $\underline{R}_2$ and the enlargement ratio. The alternate dependent variables in this figure involve C_B, which is a function of A_2/A_1 alone, and C_f, which is a function of $\underline{R}_2$ alone. Neither coefficient depends on the results of the abrupt-enlargement tests, but the resulting diagram is useful as a means of interpreting the results shown on Figures 18 and 19.

Figure 21 combines the best features of Figures 18, 19, and 20 as a dimensionless representation of the disagreement between the alternative definitions of the enlargement and boundary-friction loss coefficients. The failure of the data to show any correlation with either the enlargement ratio or the Reynolds number in this figure is an indication that the disagreement is largely due to experimental errors. From this figure it is apparent that the maximum relative difference between C_f and C_f' or C_B and C_x is about 8 percent and the average relative difference is only about 3 percent.

The customary procedure for determining the total energy loss due to abrupt enlargements consist of adding the enlargement loss (H_B) to the boundary-resistance loss (H_f). Thus, the quantity ($C_B + C_f$) represents a total-loss coefficient for the 25-diameter reach as ordinarily it would be computed. The coefficient C_L, on the other hand, is the total-loss coefficient determined from the writer's experiments. Thus, the ratio $(C_B + C_f)/C_L$ is a measure of the adequacy of the computation procedure customarily used to evaluate the total loss of energy due to the enlargement. This ratio is shown as the dependent variable on Figure 22.

The maximum disagreement between the alternate definitions of the total-loss coefficient is about 8 percent and the average disagreement is about 3 percent. If the tests made with the sleeve are disregarded, and if the tests on the smallest enlargement ratios are assumed to be subject to the largest experimental error, the results shown on Figure 22 appear to indicate that, for abrupt enlargements in smooth pipes, the computed quantity $(C_B + C_f)$ is less than 2 percent larger than the coefficient C_L determined from the experiments. In other words, the probable error in the customary computation procedure is less than 2 percent.

The similarity of Figures 21 and 22 is more than coincidental. It can be shown that the ordinate values on Figure 22 are equal to 1 (one) minus the ordinate values of Figure 21. Nevertheless, the two figures are separately justified as significant representations of the most important results obtained from the investigation.

CHAPTER VI

CONCLUSIONS

The customary procedure for computing the total energy loss in a pipe line containing an abrupt enlargement is to add the loss computed from the Borda equation to the boundary-resistance loss for uniform flow. From the results of the experiments performed for this investigation, it can be concluded that the customary procedure will give results which are as accurate as is justified by the measurements on which the computations are based. For values of the enlargement ratio greater than 2.32 the loss computed by the Borda equation is only 2 to 3 percent larger than the difference between the measured total loss and the computed boundary resistance loss. For comparison it is generally acknowledged that 5 percent is an acceptable tolerance for the estimation of boundary resistance coefficients for new, commercial pipes.

In general, the experimental results confirm the hypothesis that the total energy loss is reduced by boundary roughness in the region immediately downstream from the enlargement. Additional research on rough pipes will be required to resolve the uncertainties regarding this conclusion.

A P P E N D I X

Table 1. Location of Pipe Piezometers

Number	Distance from Enlargement	
	Feet	L/D_2
1	Located in nozzle upstream of enlargement	
2	0.189	0.741
3	0.359	1.408
4	0.525	2.059
5	1.030	4.039
6	2.030	7.961
7	4.030	15.804
8	6.035	23.667
9	8.035	31.510
10	10.045	39.392
11	12.046	47.239
12	14.051	55.102
13	16.054	62.957
14	18.060	70.824
15	19.655	77.078

Table 2. Summary of Tests on Abrupt Enlargements**

Test No.	$\frac{A_2}{A_1}$	Q	$\frac{R_2}{10^4}$	$\frac{V_1^2}{2g}$	$\frac{V_2^2}{2g}$	$\frac{h}{V_2^2/2g}$	h $\cancel{\frac{h}{V_2^2/2g}}$	C_L	C_B	C_f'	C_f	C_x
(1)	(2)	(3)	(4)	(5)	(6)	(7)	(8)	(9)	(10)	(11)	(12)	(13)
1	1.487	0.616	30.5	5.016	2.269	0.550	1.248	0.660	0.237	0.423	0.381	0.279
2	1.487	0.447	22.1	2.641	1.195	0.549	0.656	0.661	0.237	0.424	0.402	0.259
3	1.487	0.288	14.3	1.096	0.496	0.510	0.253	0.700	0.237	0.463	0.436	0.264
4	1.487	0.223	11.0	0.657	0.298	0.500	0.149	0.710	0.237	0.473	0.460	0.250
5	1.487	0.148	7.33	0.290	0.131	0.468	0.061	0.742	0.237	0.505	0.501	0.241
6	1.487	0.108	5.35	0.154	0.070	0.459	0.032	0.750	0.237	0.513	0.540	0.210
7	1.487	0.076	3.76	0.076	0.035	0.391	0.013	0.821	0.237	0.584	0.583	0.238
8	1.487	0.709	35.5	6.644	3.007	0.549	1.651	0.661	0.237	0.427	0.374	0.287
9	1.487	1.324	66.2	23.170	10.485	0.603	6.322	0.607	0.237	0.433	0.350	0.257
10	1.487	0.617	30.1	5.032	2.277	0.570	1.298	0.640	0.237	0.403	0.383	0.257
11	1.487	0.365	18.1	1.758	0.796	0.550	0.438	0.659	0.237	0.422	0.408	0.251
12	1.487	0.251	12.4	0.834	0.377	0.520	0.196	0.692	0.237	0.471	0.450	0.242
13	1.487	0.092	4.56	0.112	0.051	0.410	0.021	0.787	0.237	0.550	0.560	0.227
14	1.487	0.057	2.82	0.043	0.020	0.400	0.008	0.765	0.237	0.528	0.620	0.145
15	1.487	0.710	35.2	6.671	3.019	0.570	1.721	0.640	0.237	0.403	0.374	0.266
16	1.487	1.318	65.2	22.961	10.390	0.620	6.442	0.590	0.237	0.353	0.355	0.235
17	2.317	1.21	59.0	47.002	8.757	2.354	20.614	2.013	1.735	0.278	0.363	1.650
18	2.317	0.93	45.4	27.766	5.173	2.302	11.908	2.066	1.735	0.331	0.370	1.696
19	2.317	0.43	21.0	5.936	1.106	2.274	2.515	2.093	1.735	0.358	0.406	1.687
20	2.317	0.22	10.7	1.554	0.290	2.150	0.623	2.210	1.735	0.475	0.463	1.747
21	2.317	0.129	6.45	0.534	0.010	2.128	0.212	2.241	1.735	0.506	0.517	1.724
22	2.317	0.291	14.8	2.719	0.507	2.204	1.117	2.158	1.735	0.423	0.435	1.723
23	2.317	0.633	32.1	12.863	2.397	2.280	5.465	2.086	1.735	0.351	0.379	1.707
24	2.317	0.112	5.60	0.403	0.075	2.092	0.166	2.156	1.735	0.421	0.534	1.622

(continued)

Table 2. Summary of Tests on Abrupt Enlargements** (continued)

Test No.	$\frac{A_2}{A_1}$	Q	$\frac{R_2}{10^4}$	$\frac{V_1^2}{2g}$	$\frac{V_2^2}{2g}$	$\frac{h}{V_2^2/2g}$	n $\frac{h}{V_2^2/2g}$	C_L	C_B	C_f'	C_f	C_x
(1)	(2)	(3)	(4)	(5)	(6)	(7)	(8)	(9)	(10)	(11)	(12)	(13)
25	2.317	0.076	3.71	0.185	0.035	2.135	0.074	2.238	1.735	0.503	0.585	1.653
26	2.317	0.040	1.95	0.051	0.009	2.050	0.020	2.318	1.735	0.583	0.670	1.648
27	2.317	0.546	26.6	9.571	1.783	2.310	4.119	2.058	1.735	0.323	0.390	1.668
28	2.317	0.135	6.56	0.580	0.108	2.220	0.240	2.148	1.735	0.413	0.513	1.634
29	2.317	0.208	10.1	1.385	0.258	2.220	0.573	2.147	1.735	0.412	0.469	1.878
30	2.317	0.143	7.03	0.656	0.122	2.100	0.257	2.267	1.735	0.532	0.505	1.762
31	2.317	0.308	15.2	3.055	0.569	2.280	1.297	2.090	1.735	0.355	0.432	1.558
32	2.317	0.072	3.53	0.165	0.031	2.150	0.066	2.207	1.735	0.472	0.590	1.617
33	2.317	0.632	31.3	12.804	2.386	2.340	5.582	2.027	1.735	0.292	0.380	1.647
34	2.317	1.197	59.8	45.959	8.563	2.310	19.779	2.057	1.735	0.322	0.363	1.694
35*	2.317	0.538	25.6	9.296	1.730	2.040	3.529	2.334	1.735	0.599	0.393	1.941
36*	2.317	0.424	20.2	5.776	1.075	2.030	2.182	2.344	1.735	0.609	0.410	1.934
37*	2.317	0.272	12.9	2.378	0.443	2.020	0.894	2.353	1.735	0.618	0.446	1.907
38*	2.317	0.211	10.0	1.431	0.266	2.060	0.549	2.309	1.735	0.574	0.470	1.839
39*	2.317	0.114	5.45	0.421	0.078	1.990	0.156	2.389	1.735	0.654	0.537	1.852
40*	2.317	0.105	5.00	0.354	0.066	1.960	0.129	2.410	1.735	0.675	0.548	1.862
41*	2.317	0.074	3.51	0.175	0.033	1.900	0.062	2.456	1.735	0.721	0.591	1.865
42*	2.317	0.622	29.6	12.423	2.312	2.020	4.670	2.354	1.735	0.619	0.385	1.969
43*	2.317	0.534	26.1	9.167	1.708	2.030	3.467	2.338	1.735	0.603	0.391	1.947
44*	2.317	0.208	10.1	1.383	0.258	2.020	0.521	2.344	1.735	0.609	0.470	1.874
45*	2.317	0.102	4.98	0.335	0.062	1.940	0.121	2.436	1.735	0.601	0.548	1.888
46	4.161	0.370	18.4	14.157	0.818	6.090	4.979	10.226	9.990	0.236	0.418	9.808
47	4.161	0.226	11.2	5.281	0.305	6.040	1.842	10.279	9.990	0.289	0.459	9.820
48	4.161	0.156	7.76	2.521	0.146	6.060	0.882	10.254	9.990	0.264	0.530	9.724

(continued)

Table 2. Summary of Tests on Abrupt Enlargements** (continued)

Test No.	$\frac{A_2}{A_1}$	Q	$\frac{R_2}{10^4}$	$\frac{V_1^2}{2g}$	$\frac{V_2^2}{2g}$	$\frac{h}{V_2^2/2g}$	h $\cancel{\frac{h}{V_2^2/2g}}$	C_L	C_B	C_f'	C_f	C_x
(1)	(2)	(3)	(4)	(5)	(6)	(7)	(8)	(9)	(10)	(11)	(12)	(13)
49	4.161	0.111	5.40	1.267	0.073	5.980	0.437	10.347	9.990	0.357	0.538	9.809
50	4.161	0.430	23.1	19.142	1.105	6.110	6.754	10.207	9.990	0.217	0.400	9.807
51	6.483	0.244	12.2	14.941	0.355	11.010	3.908	30.104	30.06	0.044	0.450	29.654
52	6.483	0.109	5.46	2.998	0.071	10.800	0.770	30.254	30.06	0.192	0.435	29.717
53	6.483	0.186	9.29	8.678	0.207	10.930	2.257	30.092	30.06	0.032	0.478	29.614
54	6.483	0.142	8.00	5.068	0.121	10.930	1.318	30.091	30.06	0.031	0.493	29.598
55	6.483	0.078	3.88	1.510	0.036	10.820	0.388	30.251	30.06	0.191	0.580	29.671
56	6.483	0.036	1.80	0.325	0.008	10.570	0.082	30.401	30.06	0.341	0.678	29.723
57	6.483	0.286	14.3	20.590	0.490	11.100	5.439	29.920	30.06	-0.14	0.438	29.482
58*	6.483	0.247	11.9	15.271	0.363	11.530	4.189	29.500	30.06	-0.56	0.453	29.047
59*	6.483	0.082	3.98	1.705	0.041	11.540	0.468	29.473	30.06	-0.59	0.578	28.895
60*	6.483	0.029	1.39	0.208	0.005	11.210	0.056	29.637	30.06	-0.42	0.710	28.927
61*	6.483	0.290	14.2	21.199	0.504	11.650	5.876	29.379	30.06	-0.68	0.438	28.941
62	9.276	0.024	1.18	0.305	0.004	16.030	0.057	68.868	68.50	0.368	0.730	68.138
63	9.276	0.069	3.41	2.482	0.029	16.700	0.482	68.343	68.50	-0.16	0.596	67.747
64	9.276	0.107	5.28	5.928	0.069	16.750	1.154	68.297	68.50	-0.20	0.540	67.757
65	9.276	0.148	7.31	11.213	0.130	17.030	2.219	68.028	68.50	-0.47	0.502	67.526
66	9.276	0.200	9.90	20.587	0.239	17.380	4.154	67.757	68.50	-0.74	0.470	67.287
67	9.276	0.424	21.2	92.695	1.077	16.960	18.266	68.108	68.50	0.58	0.405	67.703
68	16.535	0.042	2.15	2.930	0.011	33.440	0.358	239.35	241.33	-1.98	0.655	238.69
69	16.535	0.074	3.77	9.056	0.033	34.260	1.134	238.34	241.33	-2.99	0.583	237.76
70	16.535	0.085	4.34	11.815	0.043	35.120	1.517	237.38	241.33	-3.95	0.566	236.71

(continued)

Table 2. Summary of Tests on Abrupt Enlargements** (continued)

Test No.	$\frac{A_2}{A_1}$	Q	$\frac{R_2}{10^4}$	$\frac{V_1^2}{2g}$	$\frac{V_2^2}{2g}$	$\frac{h}{V_2^2/2g}$	h $\cancel{\frac{h}{V_2^2/2g}}$	C_L	C_B	C_f'	C_f	C_x
(1)	(2)	(3)	(4)	(5)	(6)	(7)	(8)	(9)	(10)	(11)	(12)	(13)
71	16.535	0.107	5.44	18.613	0.068	36.510	2.486	235.88	241.33	-5.45	0.538	235.34
72*	16.535	0.088	4.26	12.738	0.047	37.480	1.747	234.86	241.33	-6.47	0.569	234.29
73*	16.535	0.059	2.85	5.687	0.021	37.240	0.775	235.14	241.33	-5.19	0.619	234.52
74*	16.535	0.107	5.18	18.779	0.069	39.430	2.708	232.98	241.33	-8.35	0.543	232.44

*Tests made with 6-inch sleeve located immediately downstream from the enlargement.

**Column headings are explained on page following Table 2.

EXPLANATION OF COLUMN HEADINGS (TABLE 2)

Col. 2 - The enlargement ratio, in which A_1 is the area of the nozzle throat and A_2 is the area of the test pipe. The pipe area (A_2) was the same for all tests.

Col. 3 - Measured discharge in cubic feet per second.

Col. 4 - $\underline{R}_2 = V_2D_2\rho/\mu$, the Reynolds number of the flow in the pipe, in which V_2 is the average velocity, D_2 is the diameter, ρ is the density and μ is the viscosity corresponding to the measured water temperature for each test.

Col. 5 and 6 - Velocity heads, in which V_1 is the average velocity in the nozzle throat, and V_2 is the average velocity in the test pipe.

Col. 7 - $\Delta h = (h_2 - h_1)$, in which h_1 is the piezometric head at the end of the nozzle ($L/D_2 = 0$) and h_2 is the piezometric head at a section 25 diameters downstream from the enlargement ($L/D_2 = 25$).

Col. 9 - $C_L = H_L/(V_2^2/2g)$, in which $H_L = -\Delta h + V_1^2/2g - V_2^2/2g$ = the total loss in energy head in the 25-diameter reach downstream from the enlargement.

Col. 10 - $C_B = H_B/(V_2^2/2g)$, in which H_B is the loss attributed to the enlargement from the Borda equation.

Col. 11 - $C_f' = C_L - C_B = (H_L - H_B)/(V_2^2/2g)$, a measure of the residual loss attributable to boundary resistance if the enlargement loss (Borda equation) is subtracted from the measured total loss.

Col. 12 - $C_f = H_f/(V_2^2/2g) = fL/D_2$, in which H_f is the boundary resistance loss computed from the Darcy equation, f is the normal resistance coefficient for the test pipe, and $L/D_2 = 25$.

Col. 13 - $C_x = C_L - C_f = (H_L - H_f)/(V_2^2/2g)$, a measure of the residual loss attributable to the enlargement if the normal resistance loss is subtracted from the measured total loss.

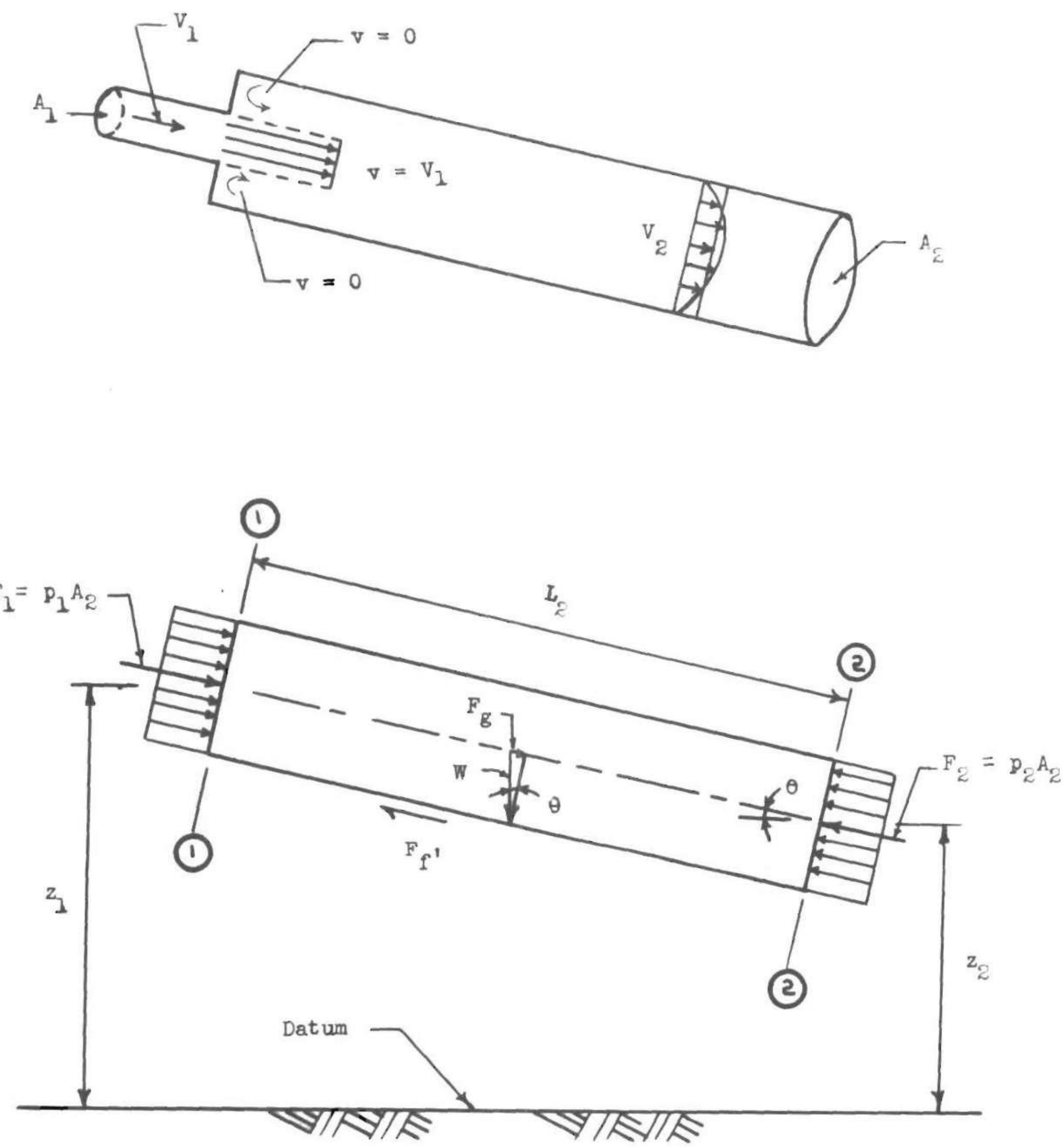

Figure 1. Definition Sketch for Flow in Abrupt Enlargements

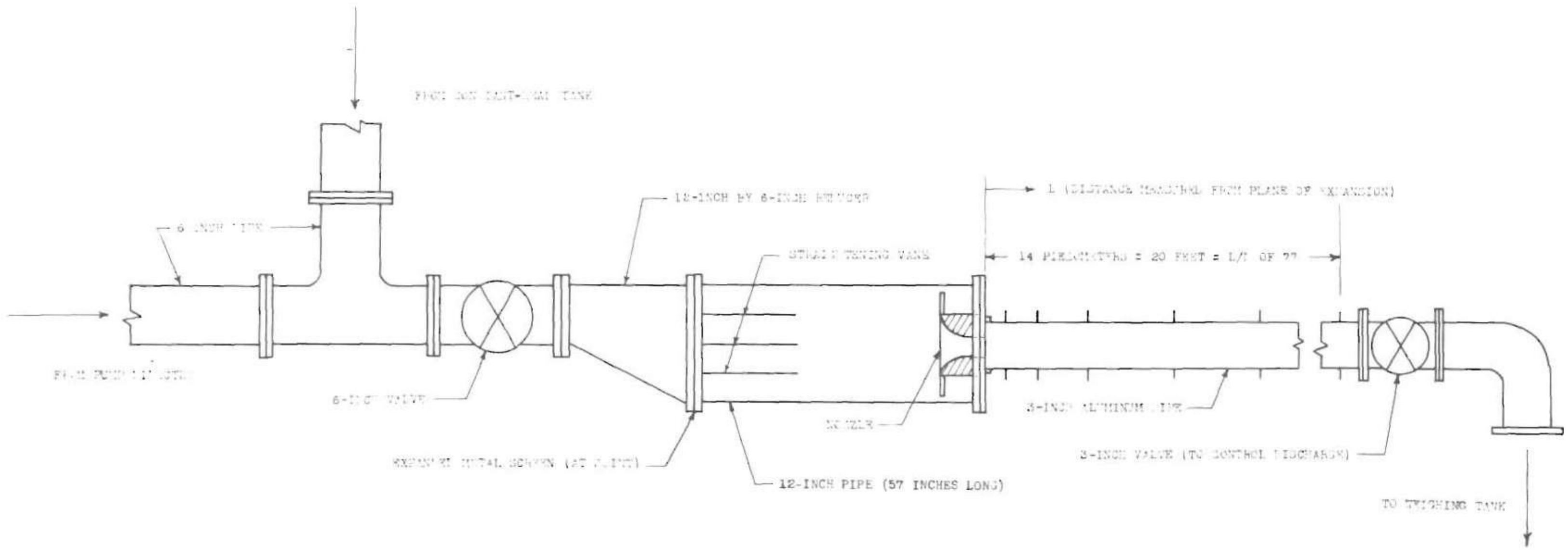

Figure 2. Laboratory Setup (Schematic)

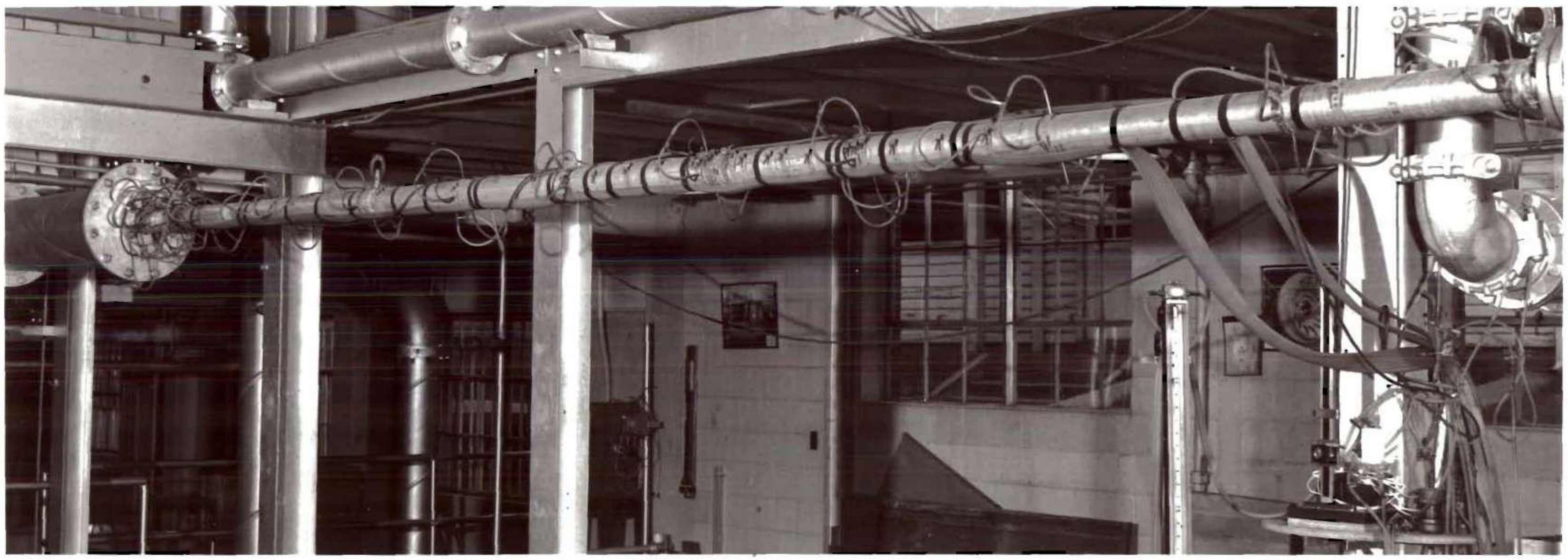

Figure 3. General View of Laboratory Equipment

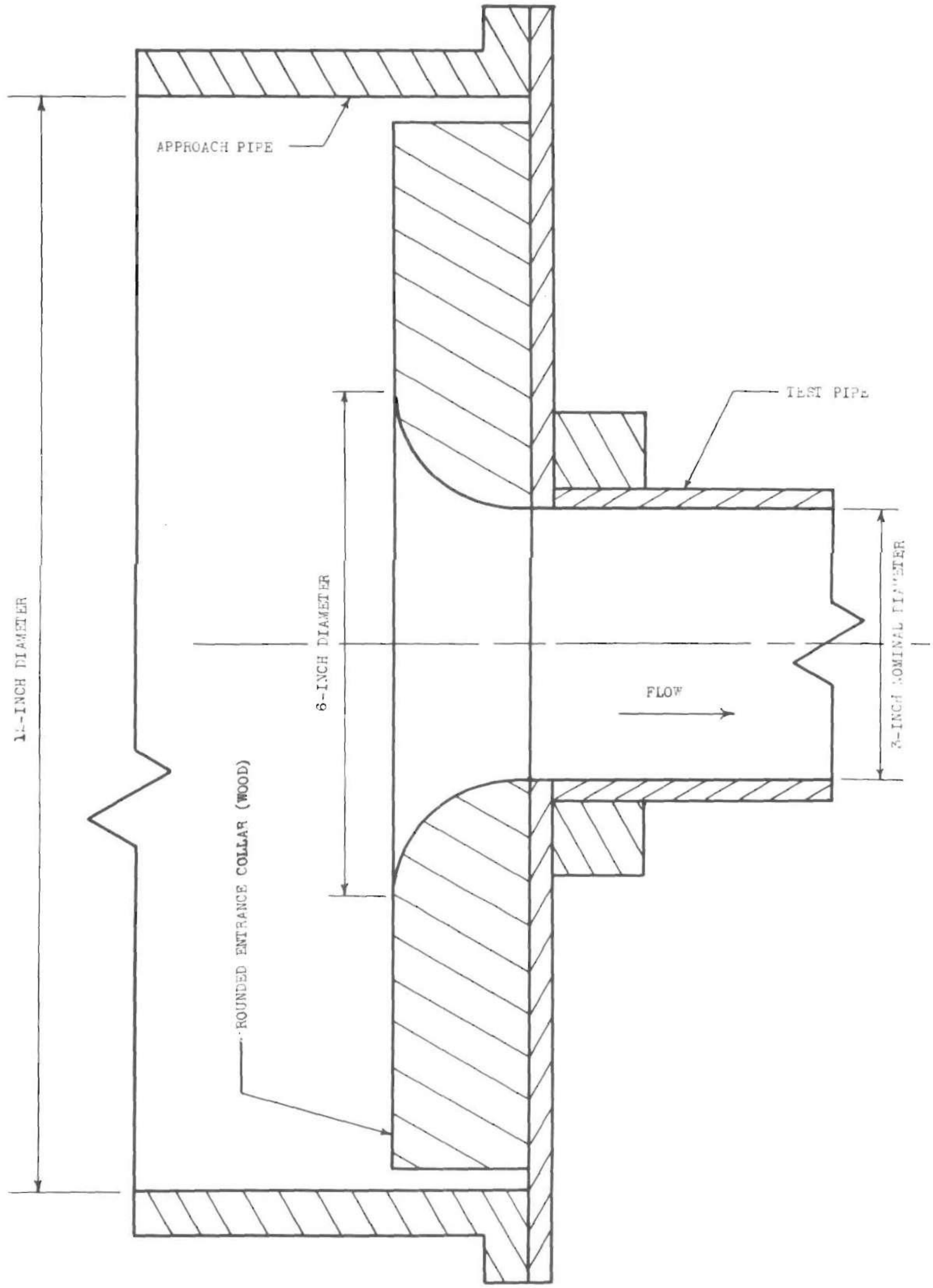

Figure 4. Entrance for Boundary Resistance Tests

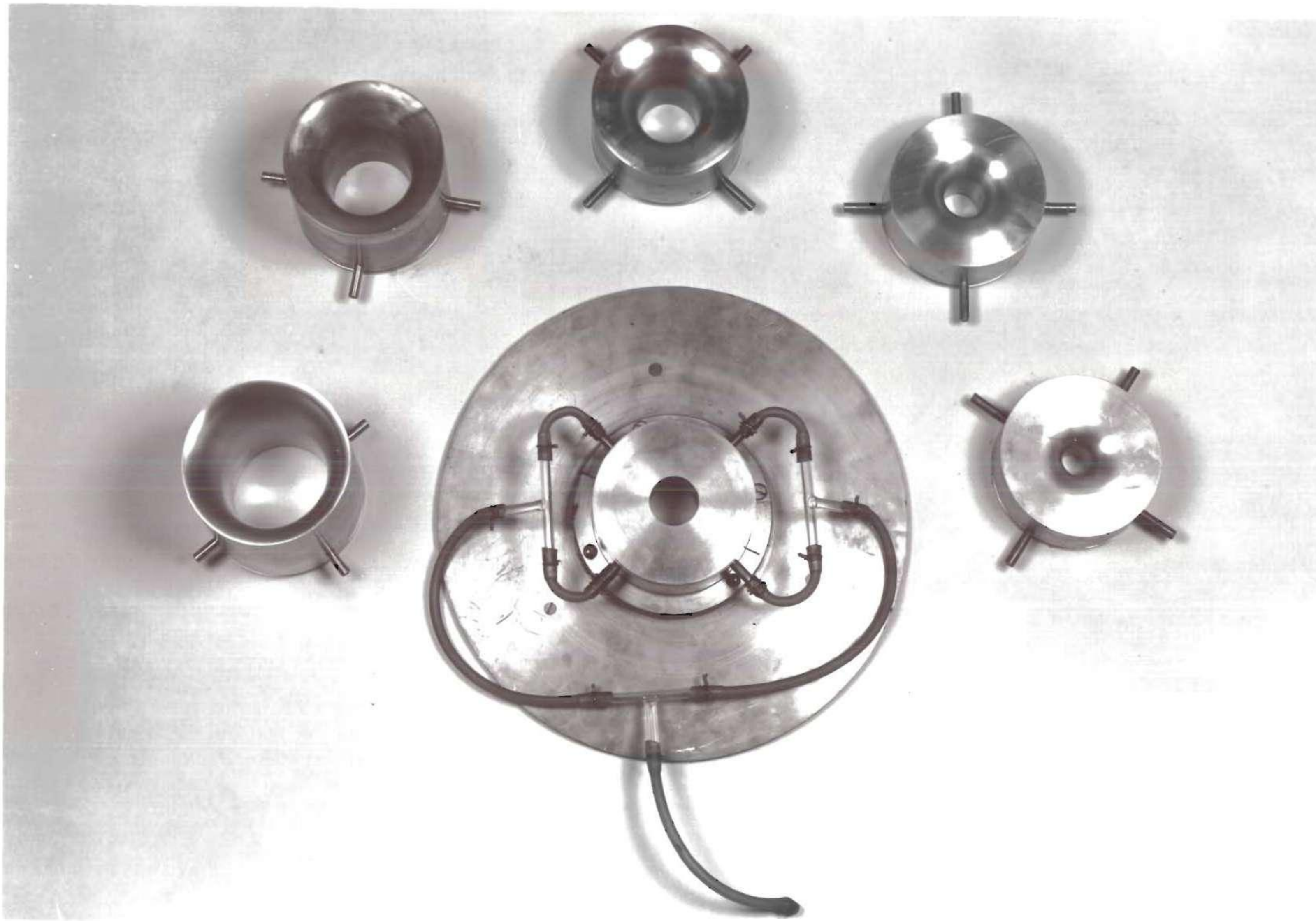

Figure 5. Nozzles Used for Enlargement Tests

ALUMINUM NOZZLE DIMENSIONS

(inches)

A_2/A_1	A	B	C	D	E	F	G
1.49	4	0.75	2.508	0.84	2.50	1.67	4.17
2.32	4	1.00	2.009	0.67	2.00	1.33	3.33
4.16	4	1.25	1.499	0.50	1.50	1.00	2.50
6.48	4	1.40	1.201	0.50	1.20	1.00	2.20
9.28	4	1.50	1.004	0.50	1.00	1.00	2.00
16.53	4	1.63	0.752	0.50	0.75	1.00	1.75

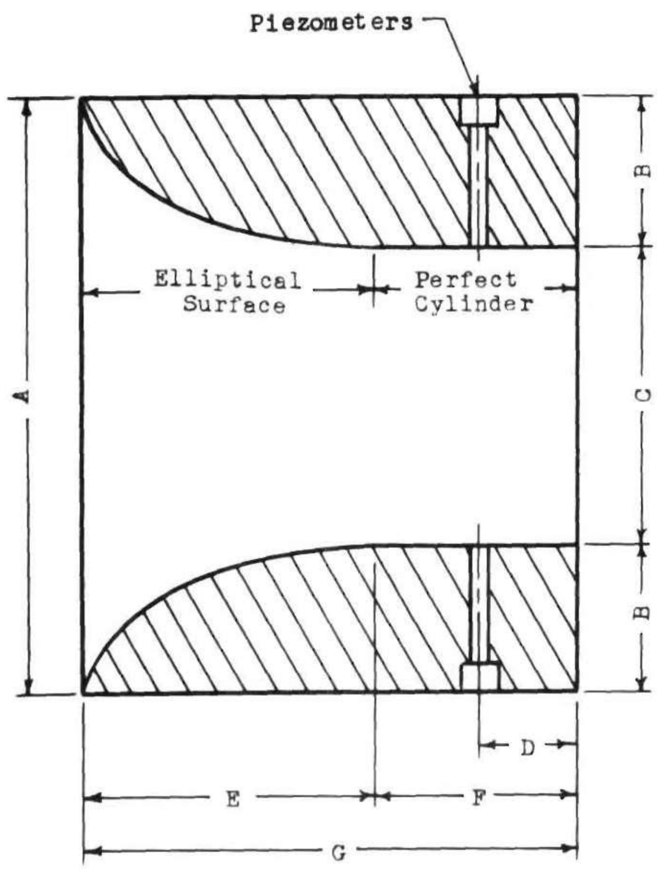

CENTERLINE SECTION

Figure 6. Dimensions of Nozzles

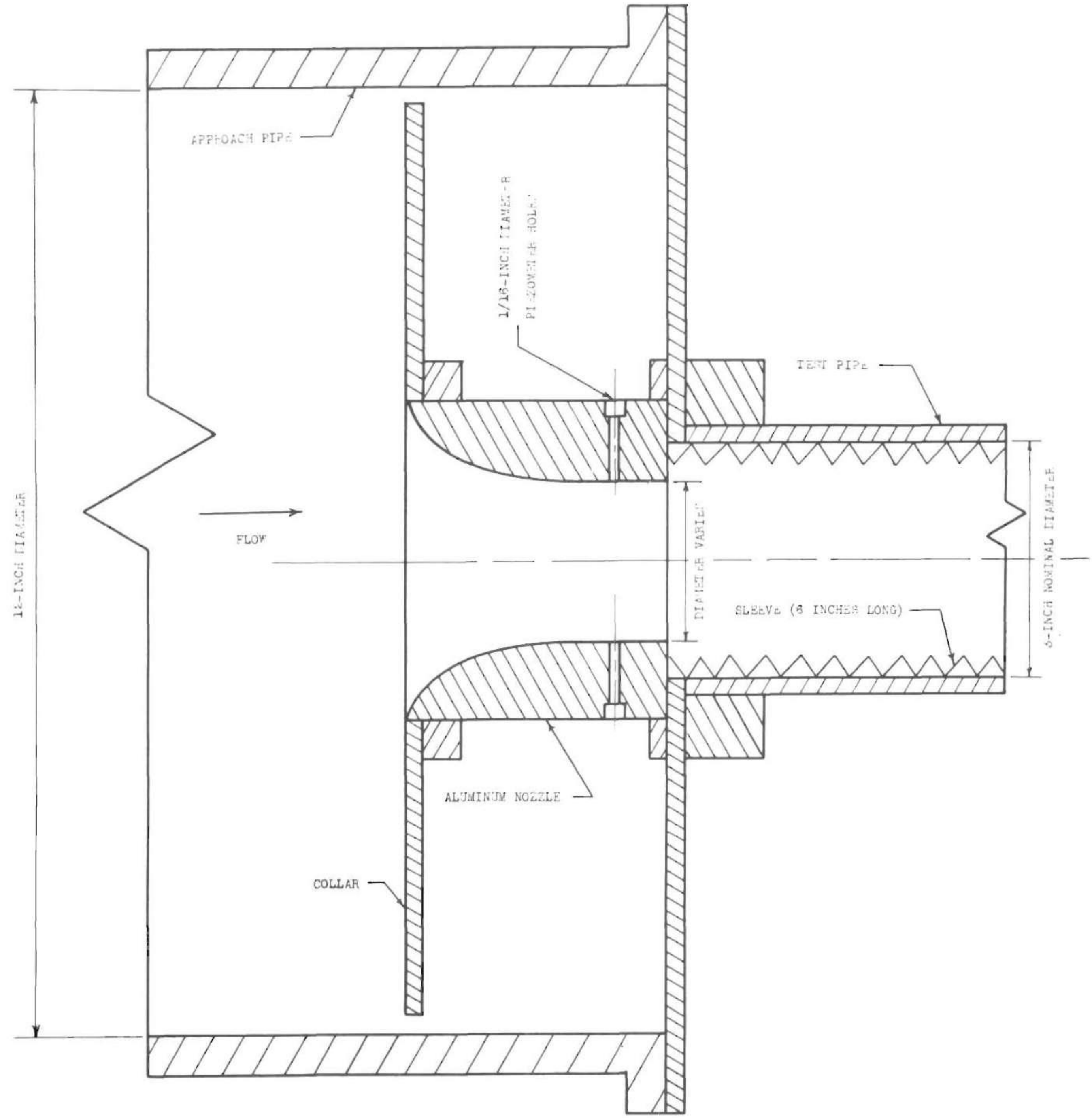

Figure 7. Entrance for Abrupt-Enlargement Tests

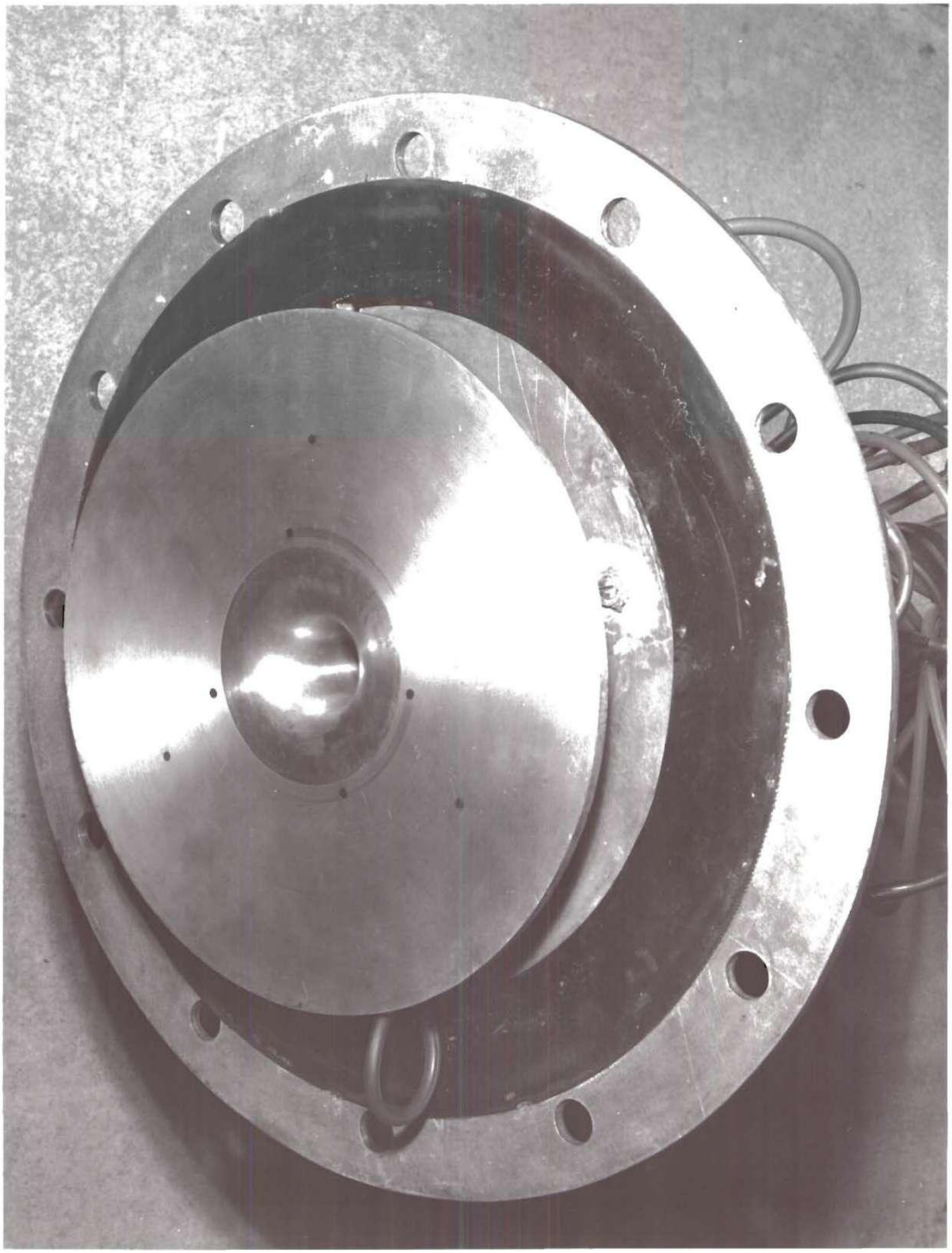

Figure 8. Typical Nozzle Installed in Entrance Section

Figure 9. Expanded-Metal Sleeve

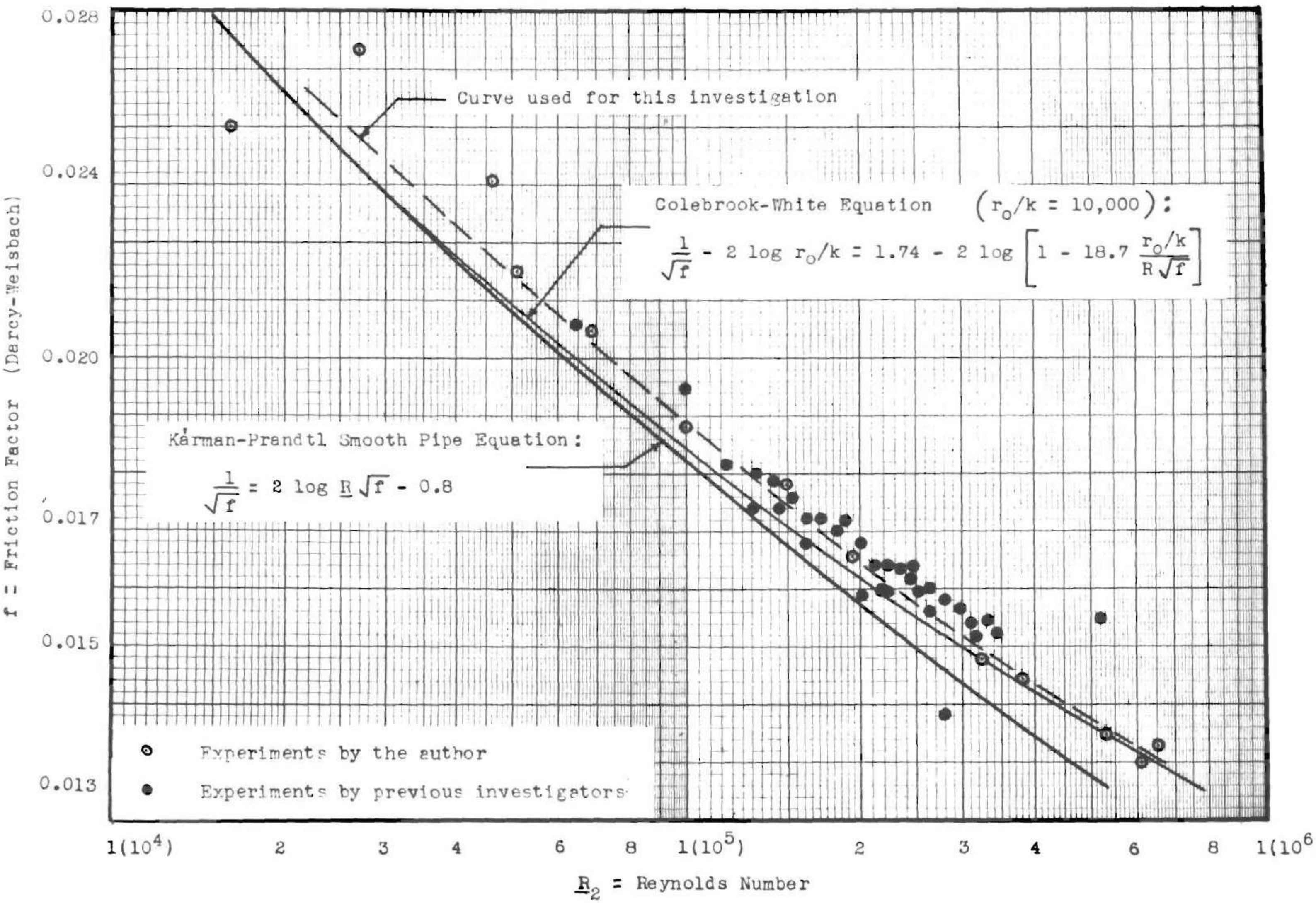

Figure 10. Results of Boundary Resistance Tests

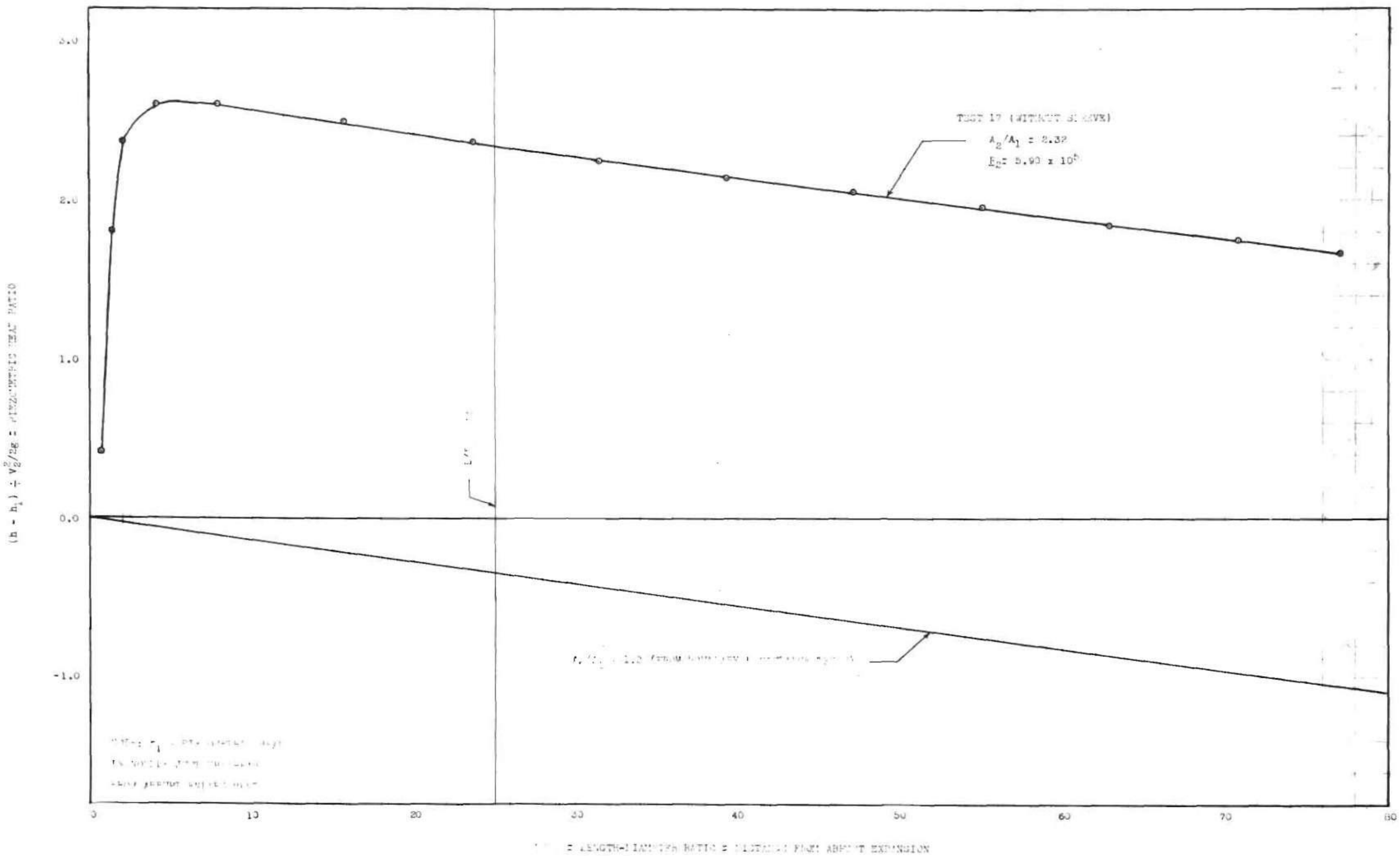

Figure 11. Piezometric Profile for Typical Enlargement Test

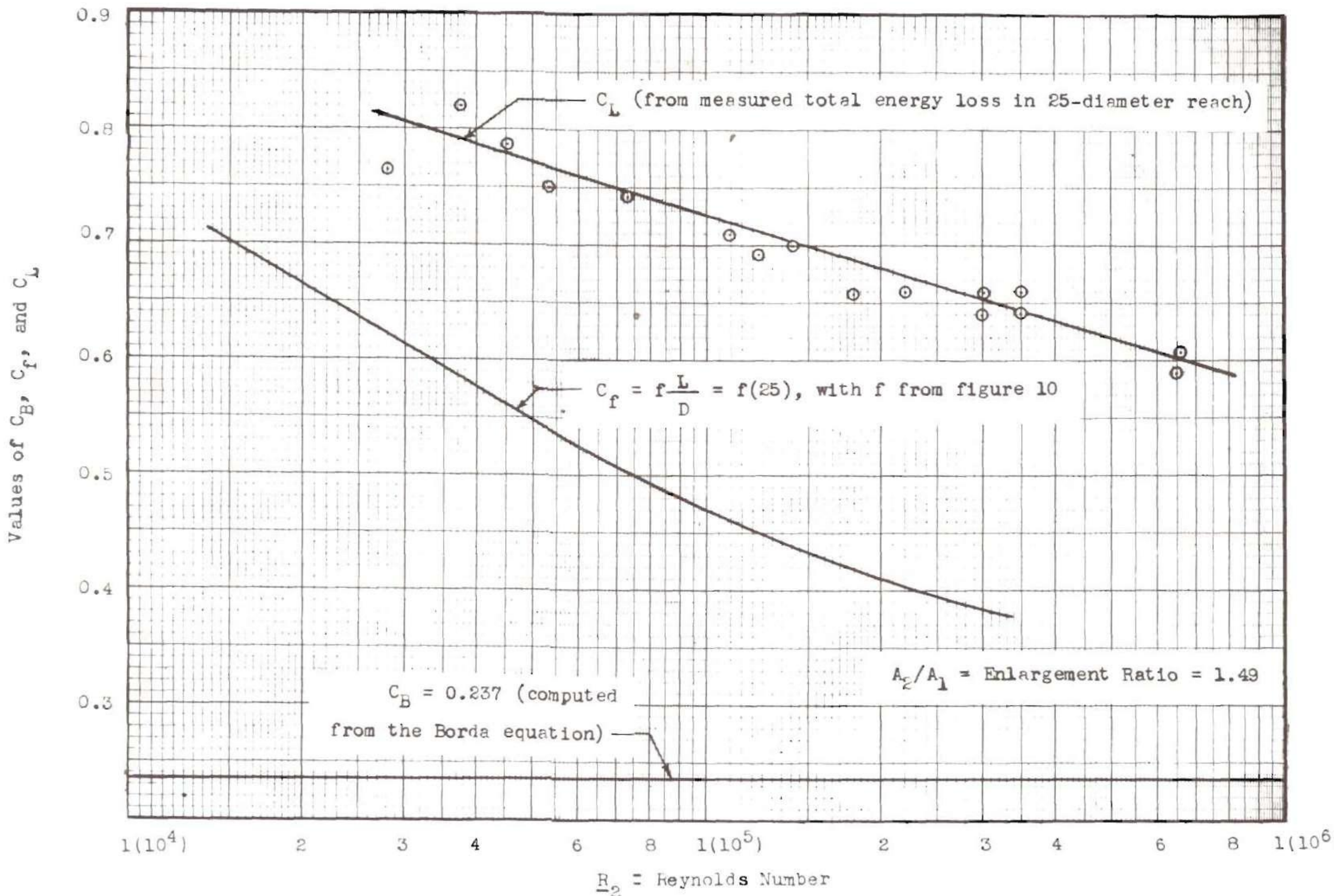

Figure 12. Total-Loss Coefficient, $A_2/A_1 = 1.49$

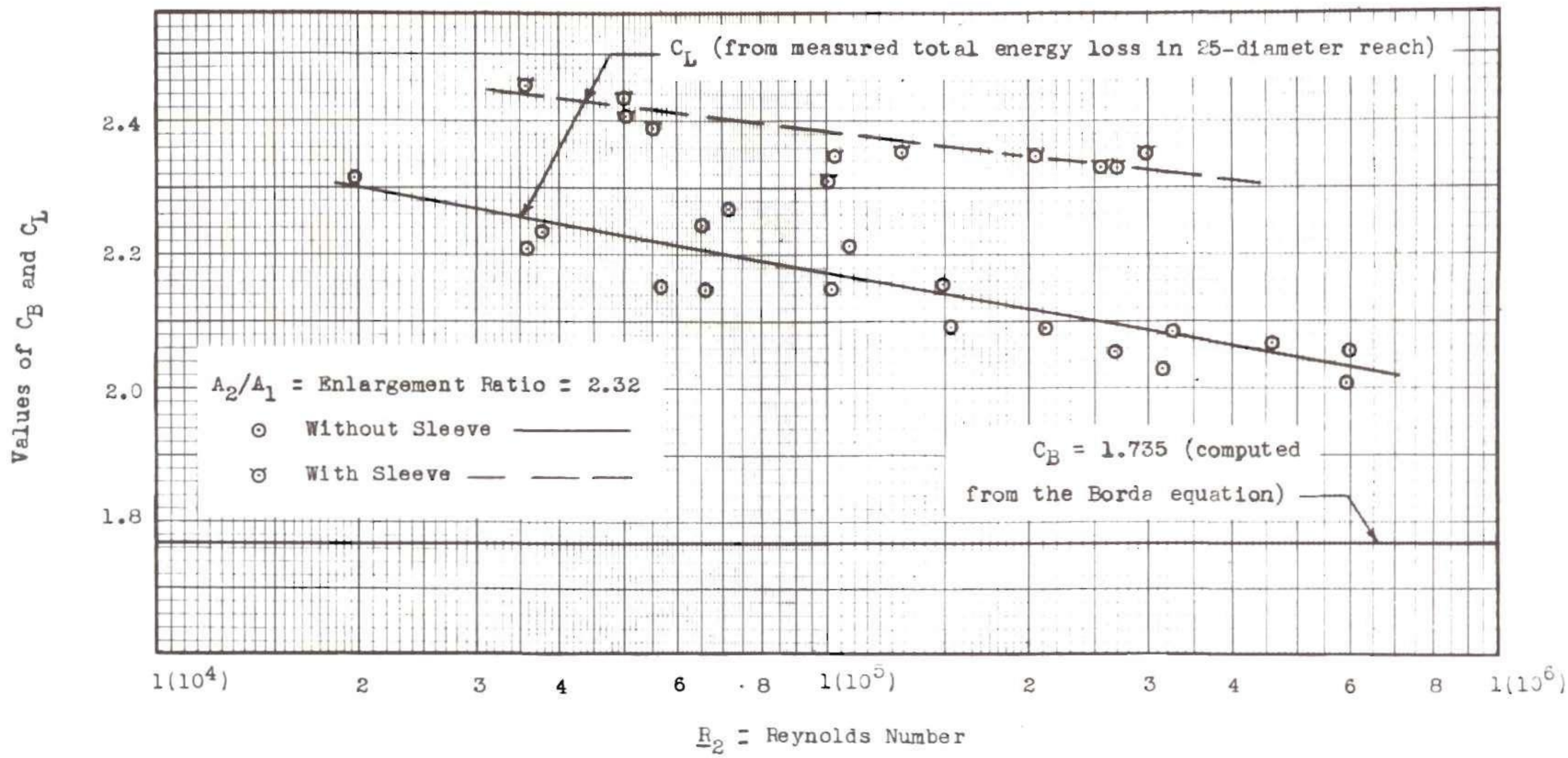

Figure 13. Total-Loss Coefficient, A_2/A_1 = 2.32

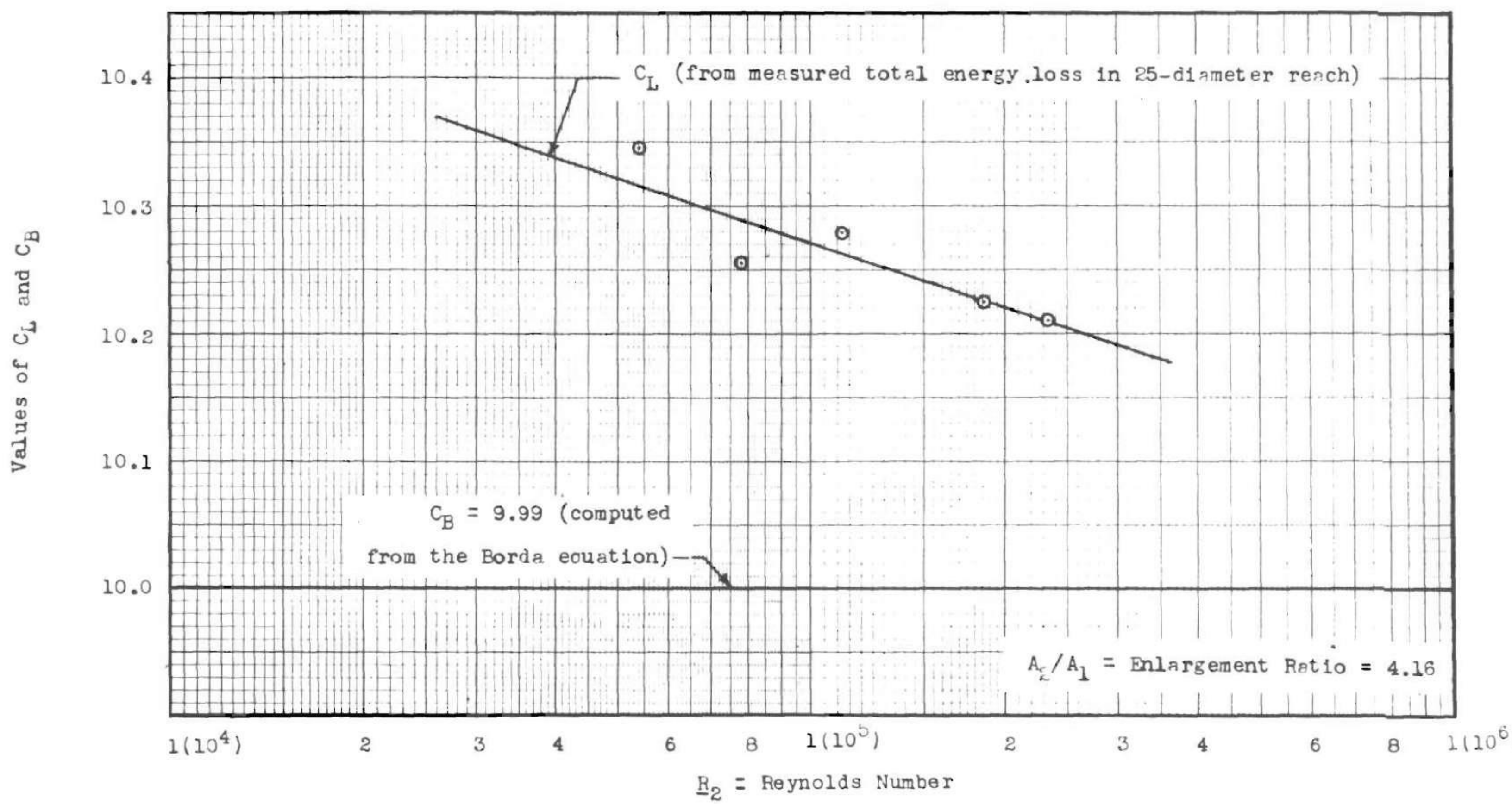

Figure 14. Total-Loss Coefficient, A_2/A_1 = 4.16

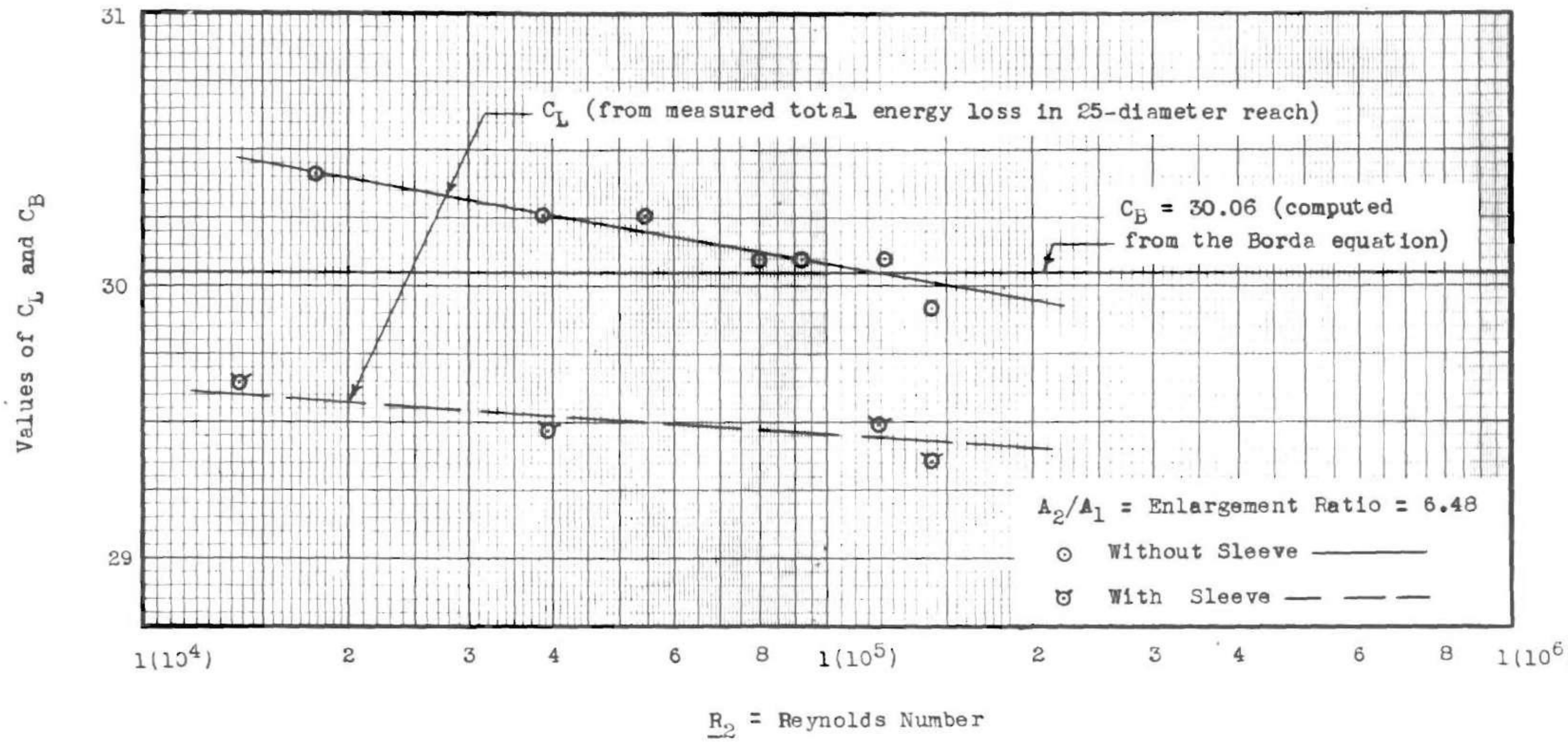

Figure 15. Total-Loss Coefficient, A_2/A_1 = 6.48

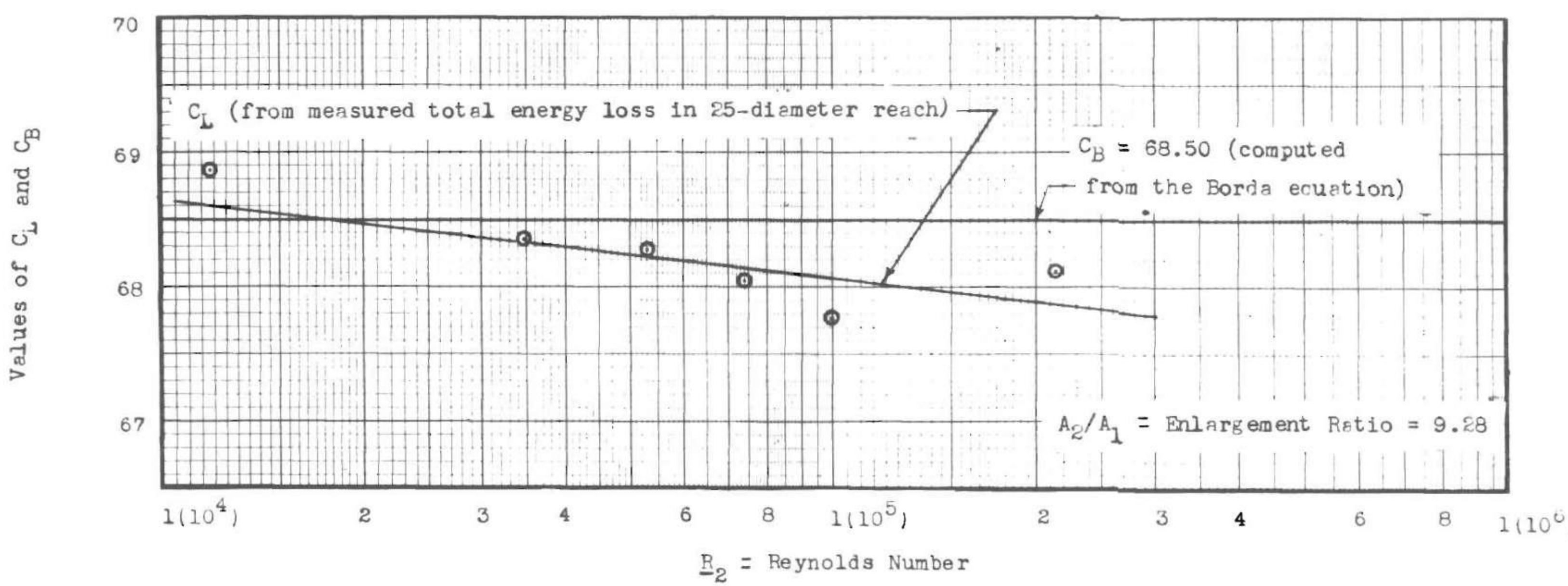

Figure 16. Total-Loss Coefficient, $A_2/A_1 = 9.28$

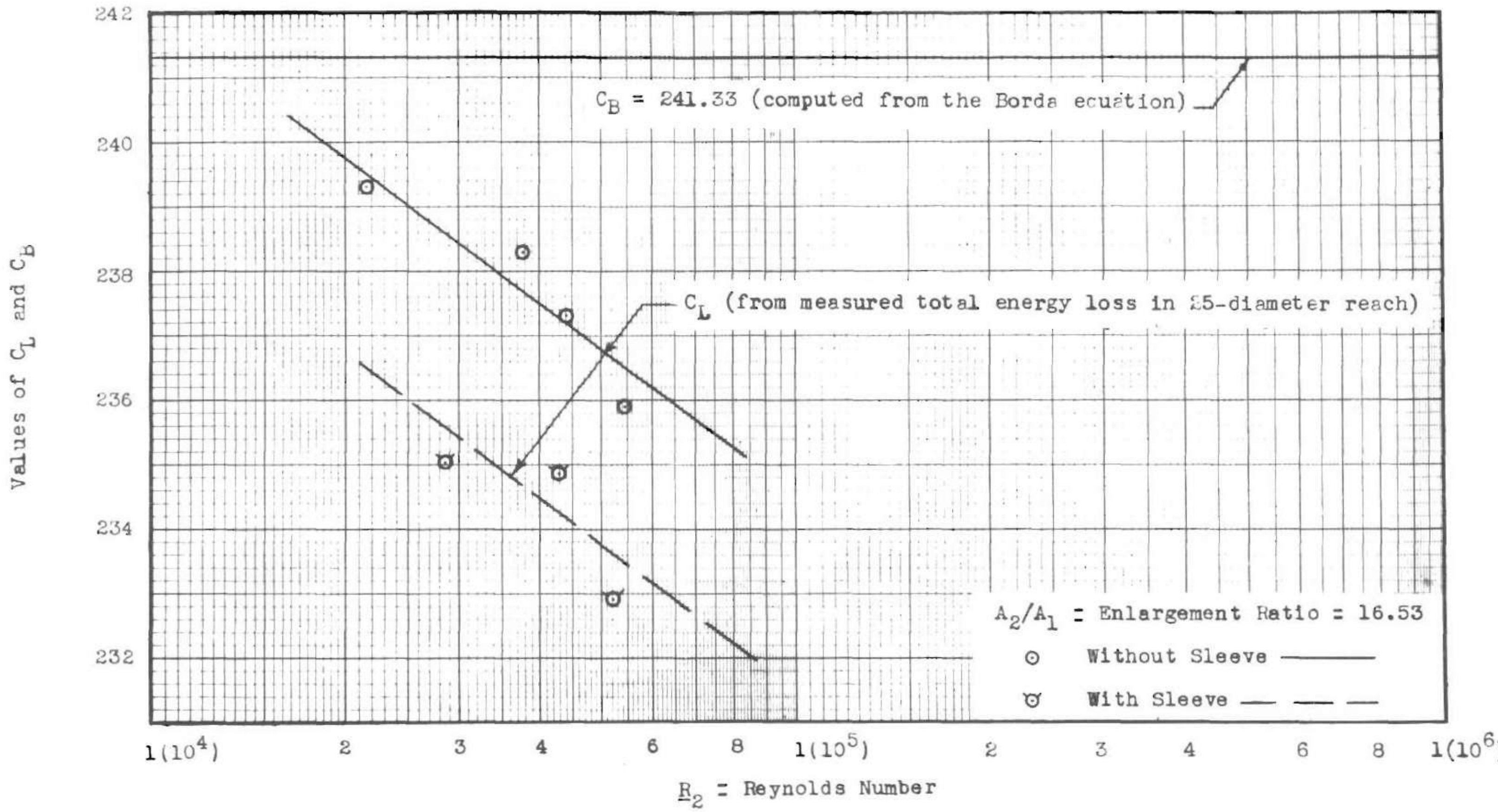

Figure 17. Total-Loss Coefficient, A_2/A_1 = 16.53

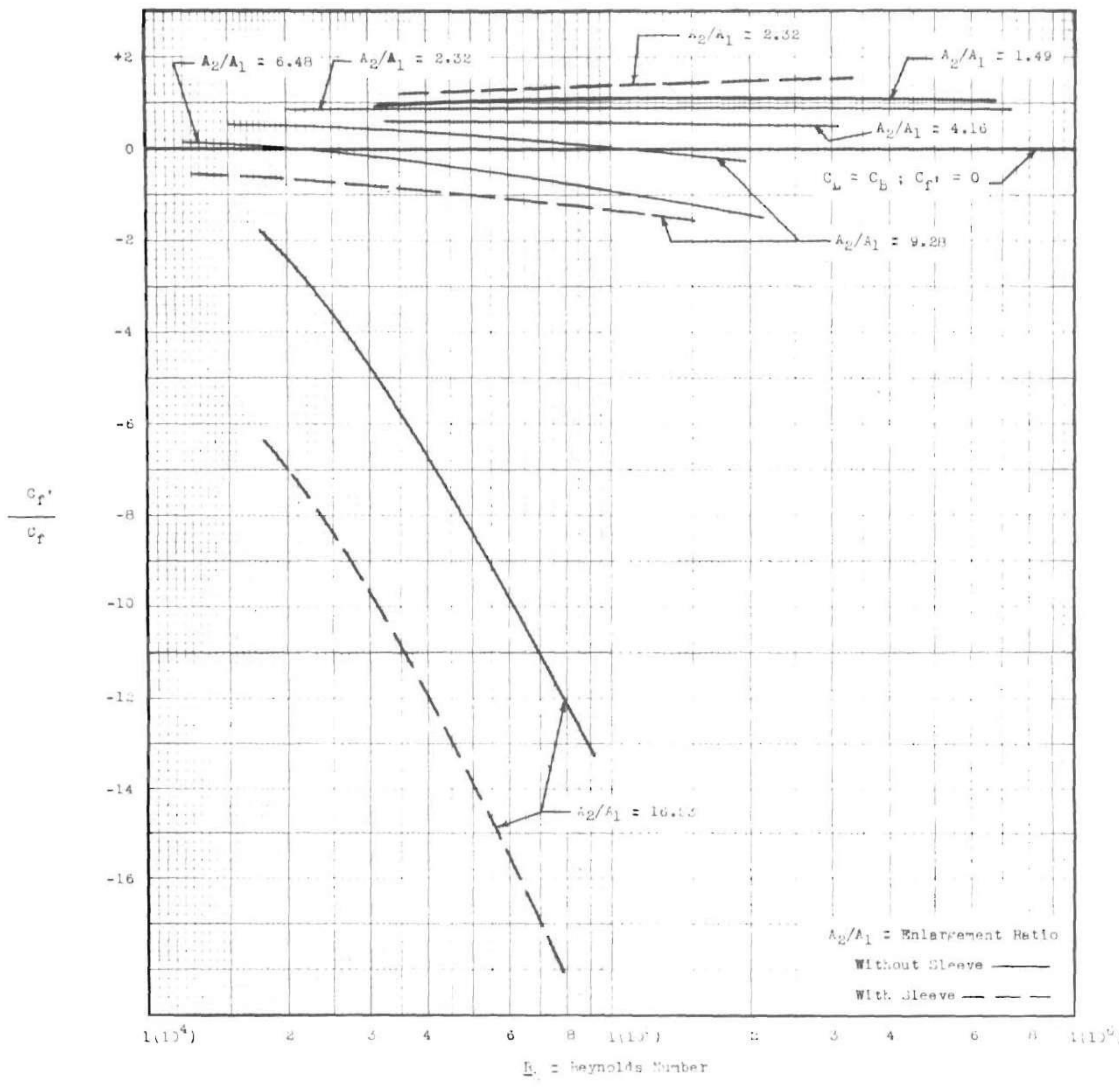

Figure 18. Ratio of Resistance Coefficients, C_f'/C_f

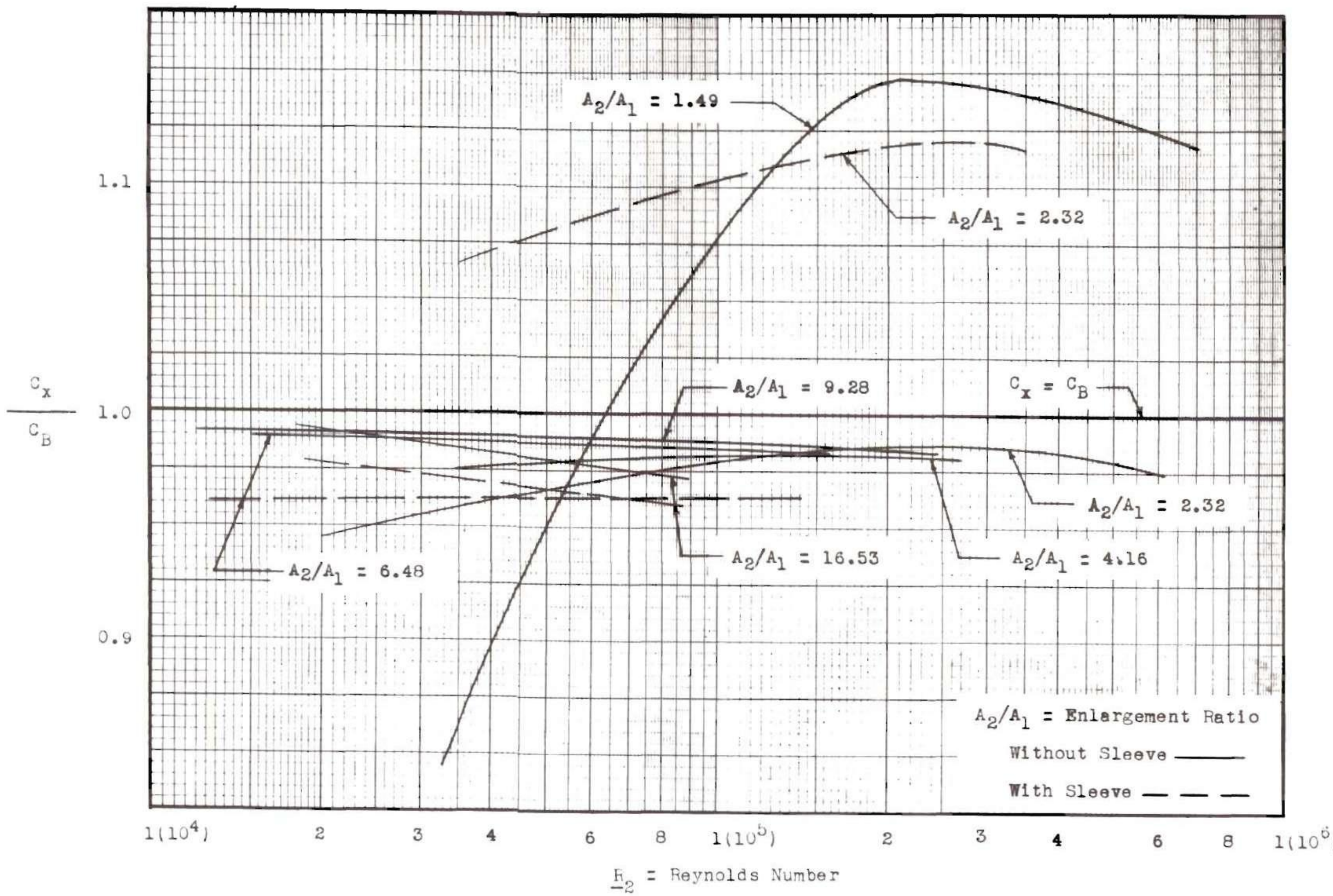

Figure 19. Ratio of Enlargement Coefficients, C_x/C_B

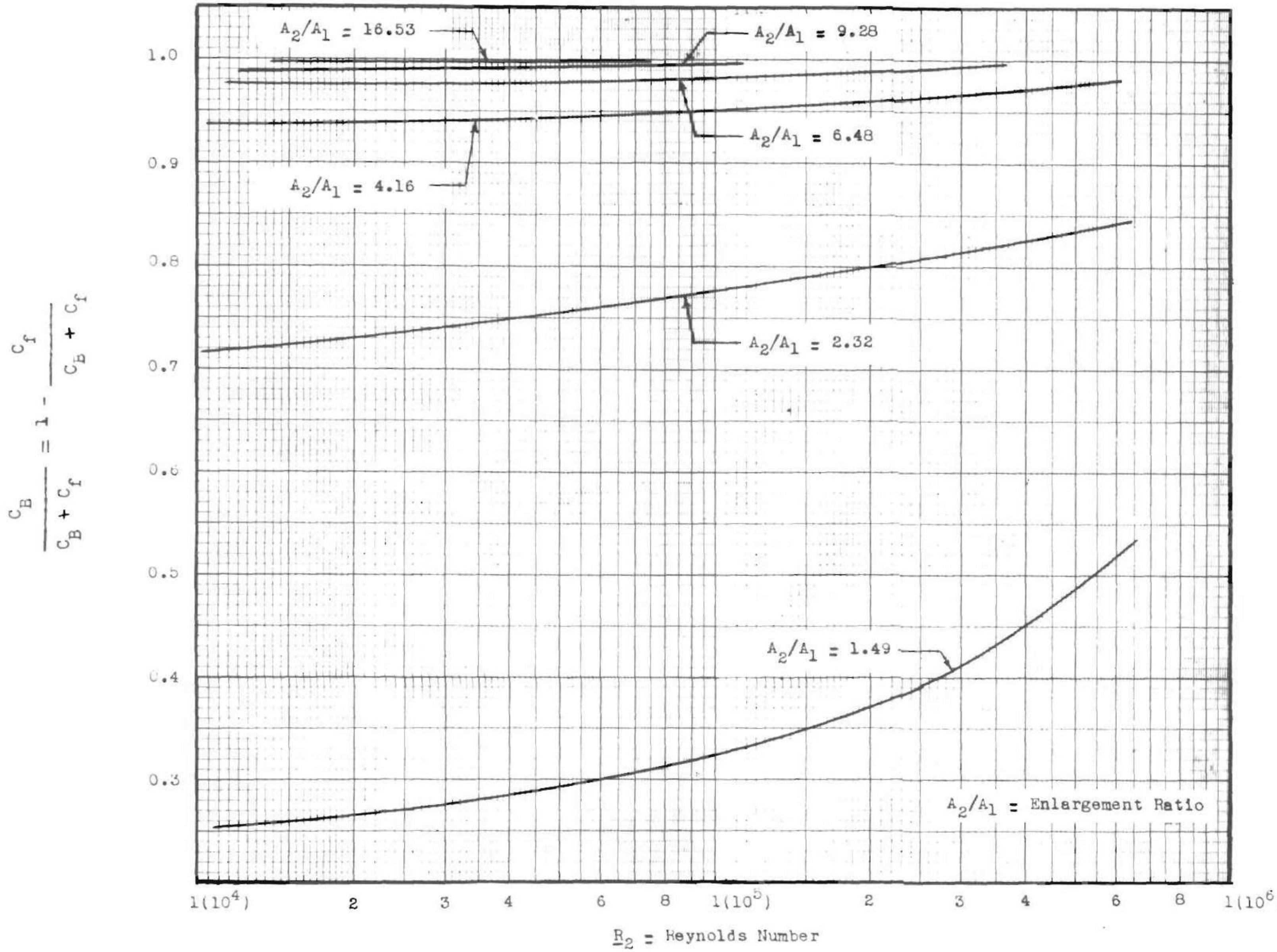

Figure 20. Ratio of Coefficients, $C_B/(C_B + C_f)$

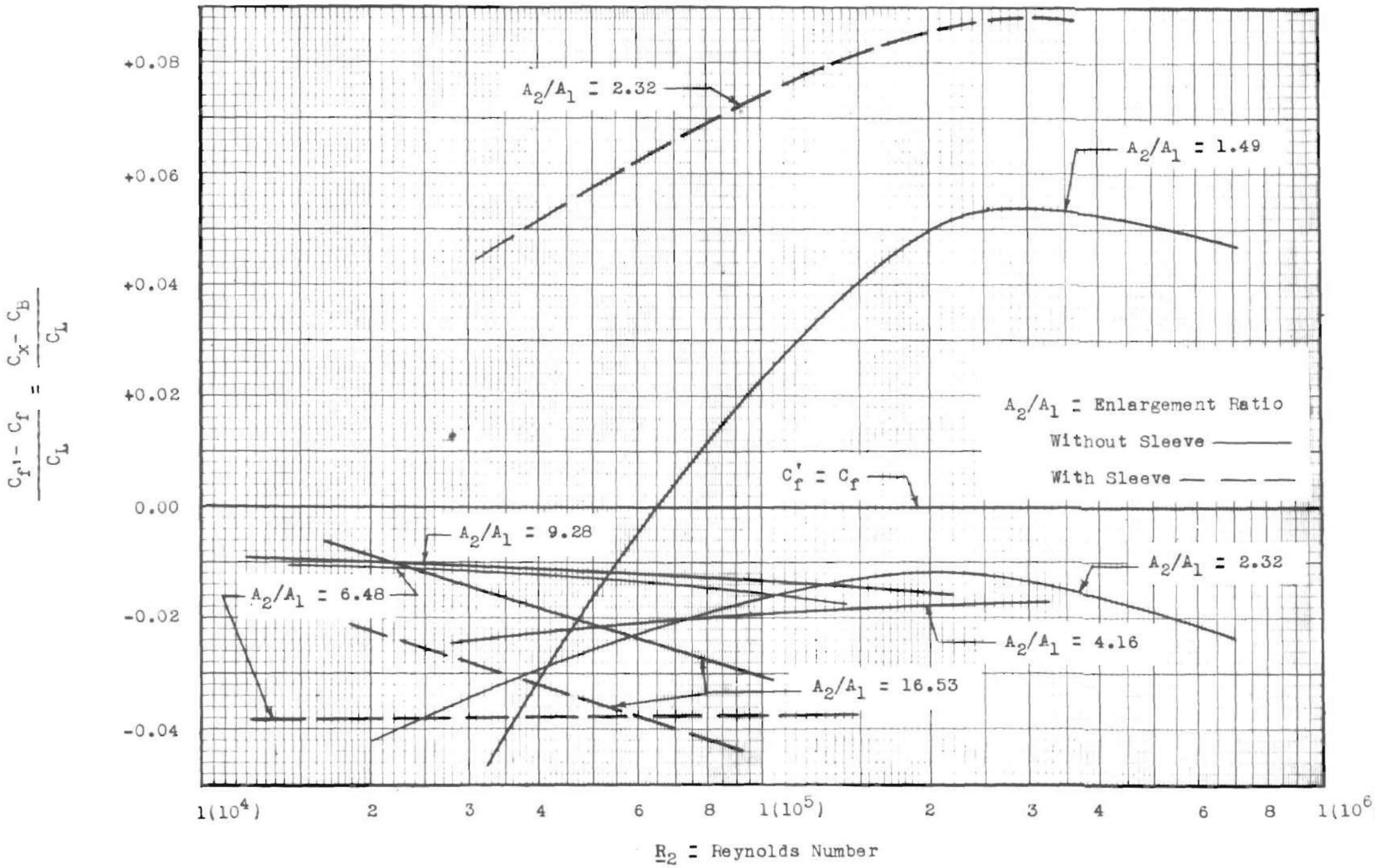

Figure 21. Ratio of Coefficients, $(C_f' - C_f)/C_L$

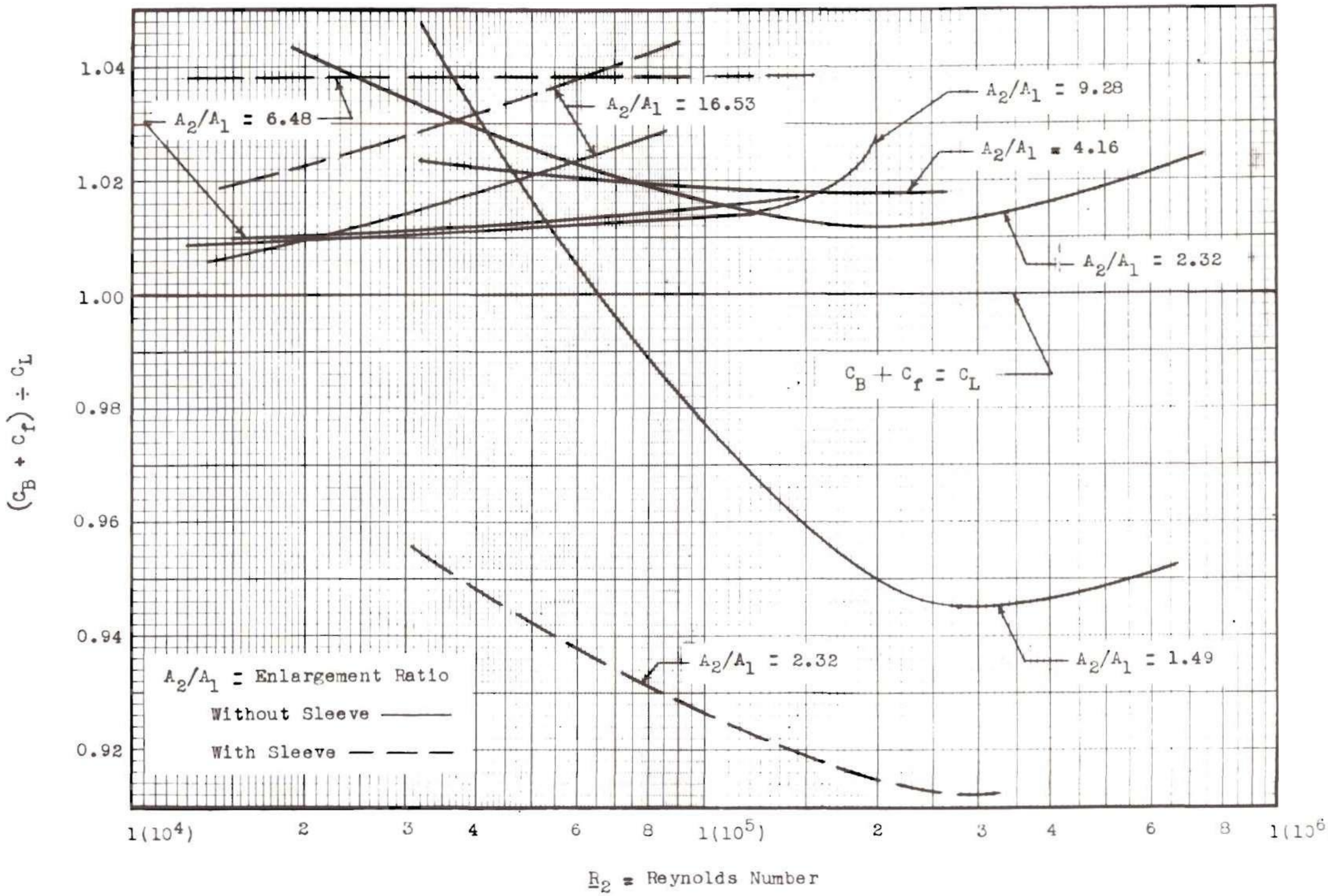

Figure 22. Ratio of Coefficients, $(C_B + C_f)C_L$

REFERENCES

(1) Gibson, A. H., "On the Resistance to Flow of Water through Pipes or Passages having Divergent Boundaries," Transactions of the Royal Society of Edinburgh, Vol. 48, Part I, No. 5, 1910, pp. 97-116.

(2) Gibson, A. H., "The Conversion of Kinetic Energy in the Flow of Water through Passages having Divergent Boundaries," Proceedings of the Royal Society of the Arts, Vol. 83, 1910, pp. 366-378.

(3) Archer, W. H., "Loss of Head Due to Enlargement in Pipes," Transactions of the American Society of Civil Engineers, Vol. 76, 1913, pp. 999-1026.

(4) Kalinske, A. A., "Conversion of Kinetic to Potential Energy in Flow Expansions," Transactions of the American Society of Civil Engineers, Vol. 111, 1946, pp. 355-390.

(5) Schütt, H., "Versuche Zur Bestimmung der Energieverluste bei plotzlicher Rohrerweiterung," Mitteilungen des Hydraulischen Instituts der Technischen Hochschule Munchen, Vol. I, 1926, pp. 45-58.

(6) Fleetwood, T. W., Jr., Abrupt Enlargements in Smooth and Rough Pipes M. S. Thesis, Georgia Institute of Technology, June 1955.

(7) Schnable, G. B., Diametric Obstructions in Pipes, M. S. Thesis, Georgia Institute of Technology, June 1953.

(8) Nikuradse, J., "Laws of Flow in Rough Pipe," Technical Memorandum 1292, National Advisory Committee for Aeronautics, 1950.

(9) Albertson, M. L., Y. B. Dai, R. A. Jensen, and H. Rouse, "Diffusion of Submerged Jets," Transactions of the American Society of Civil Engineers, Vol. 115, 1950, pp. 639-697.

(10) Hsu, H. C., Characteristics of Mean Flow and Turbulence at an Abrupt Two-Dimensional Expansion, Ph.D. Thesis, University of Iowa, February 1950.

(11) Tults, H., "Flow Expansion and Pressure Recovery in Fluids," Proceedings of the American Society of Civil Engineers, Separate 567, Vol. 80, December 1950.

(12) Moore, W. L., "The Effect of the Location of a Plane Boundary on the Diffusion of a Two-Dimensional Submerged Jet," University of Texas, Annual Report to the National Science Foundation (unpublished), 1954.

(13) Rouse, H., Elementary Mechanics of Fluids, John Wiley and Sons, New York, 1946.

(14) Shapiro, A. H., and R. D. Smith, "Friction Coefficients in the Inlet Length of Smooth Round Tubes," Technical Note No. 1785, National Advisory Committee for Aeronautics, 1948.